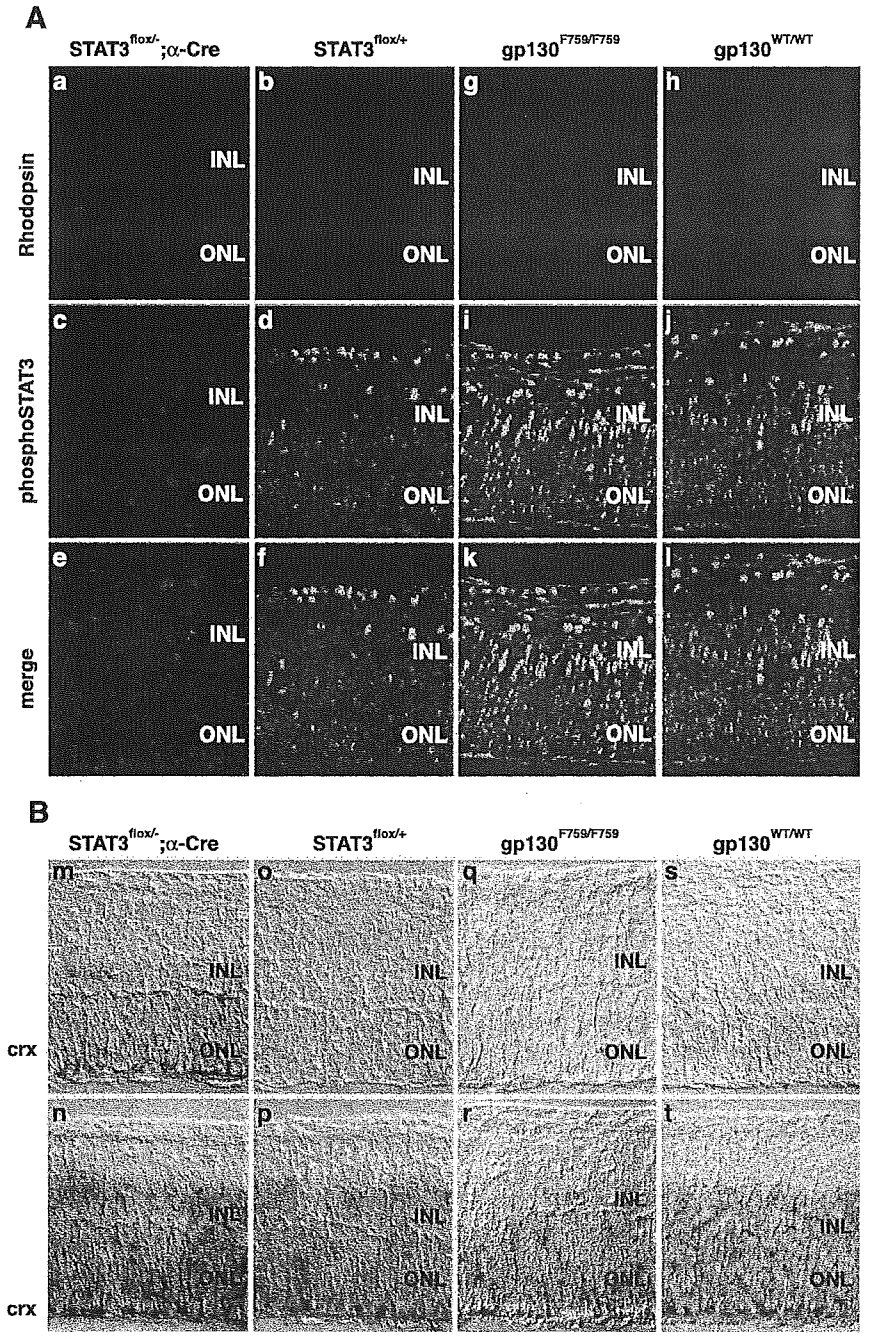

Fig. 3. Effects of CNTF on P0 retinal explants derived from CNTF/gp130 signal-deficient mice. All retinal explants were started at P0 and fixed at day 5. (A) All P0 retinal explants were cultured with CNTF. P0 retinal explants from STAT3$^{flox/-}$;α-Cre mice expressed Rhodopsin (a) and showed no STAT3 activation in most ONL cells (c). A small number of phosphoSTAT3 positive cells were occasionally seen in the ONL, but they never expressed Rhodopsin (e). By contrast, explants from STAT3$^{flox/+}$ mice, littermates of the mutant mice considered to be wild type, expressed no Rhodopsin (b) and showed STAT3 activation in the ONL (d). Merge (e, f). No STAT3 activation was detected in Rhodopsin-expressing cells. P0 retinal explants from gp130$^{F759/F759}$ mice with deficiency of SHP2 activation expressed no Rhodopsin (g) and showed STAT3 activation in the ONL (i), like P0 retinal explants prepared from wild-type littermates (h, j). Merge (k, l). (B) *crx* mRNA was highly expressed in the ONL and outer half of the INL of control P0 retinal explants (n, p, r, t). After CNTF exposure, P0 retinal explants from STAT3$^{flox/-}$;α-Cre mice clearly expressed *crx* mRNA (m), in contrast to P0 retinal explants from STAT3$^{flox/+}$ mice (o). CNTF actually decreased the *crx* mRNA expression level slightly in STAT3$^{flox/-}$;α-Cre retina, but the degree of the reduction was much smaller than that in STAT3$^{flox/+}$ retina. The relative levels of *crx* mRNA expression after CNTF exposure to the levels of each control measured by NIH image were 50% and 15% in STAT3$^{flox/-}$;α-Cre retina and STAT3$^{flox/+}$ retina, respectively. *crx* mRNA expression in P0 retinal explants from gp130$^{F759/F759}$ mice (q) and from wild-type littermates (s) were markedly reduced after CNTF exposure. The relative levels of *crx* mRNA expression to the levels of each control measured by NIH image were 5% and 13% in gp130$^{F759/F759}$ knock-in retina and wild-type retina, respectively. ONL, outer nuclear layer; INL, inner nuclear layer.

We also directly investigated whether MAPK activation is required for the inhibition by CNTF in wild-type animals by using PD098059 (Alessi et al., 1995), a specific inhibitor of MEK which is an activator of MAPK. Under standard condition in which MAPK was not activated in the presence of PD098059 (50 μM), P0 retinal explants never expressed Rhodopsin after exposure to CNTF (data not shown), further confirming that SHP2-mediated RAS/MAPK pathway is not involved in the CNTF-induced inhibition of rhodopsin expression in the postnatal retinal cells.

Blockade of STAT3-mediated signaling after starting P0 retinal explants was sufficient to override the CNTF-induced inhibitory effect on Rhodopsin expression

To exclude indirect effects of STAT3 deficiency in earlier embryonic period, we developed an efficient gene transfer system into cells in retinal explants by electroporation to attempt to block STAT3 activation only after starting retinal explants. Using this system, we introduced a dominant-negative form of STAT3 (STAT3F) at various times during development. STAT3F has a point mutation in the putative phosphorylation site, Tyr705, and it binds to the gp130 receptor, which in turn leads to competitively inhibited phosphorylation of endogenous STAT3 upon activation of the gp130 receptor (Minami et al., 1996; Nakajima et al., 1996). STAT3F gene fused with HA-tag was placed under control of the chicken beta-actin-cytomegalovirus hybrid promoter (CAG) (Niwa et al., 1991) that allows the transgenes to be expressed in all three layers including the ONL. We performed electroporation of plasmid CAG-HA-STAT3F with pCAG-EGFP, or plasmid CAG with pCAG-EGFP into the wild-type P0 retinal explants. The explants prepared from wild-type P0 retina were immediately subjected to electroporation of these constructs and then exposed to CNTF (50 ng/ml). At day 1, green fluorescence elicited by EGFP was already detected under a dissecting fluorescence microscope. Since the STAT3F gene was regulated under the same promoter, we assumed that expression of STAT3F had already started by day 1. The intensity of the green fluorescence increased for the first several days until it reached the peak level at around day 7, after which it persisted until at least day 10. We fixed the explants at day 7 and examined frozen sections of them. The cells into which STAT3F had been successfully introduced by electroporation were recognized by either green fluorescence or anti-HA immunostaining, and they were widely distributed throughout all three layers in the retinal explant (Fig. 4Aa). HA-tag fused with STAT3F was mainly in the cytoplasm, which is consistent with the fact that unphosphorylated STAT3 cannot be translocated into the nucleus (Takeda and Akira, 2000). After electroporation of plasmid CAG-HA-STAT3F with pCAG-EGFP, Rhodopsin-expressing cells were found even in the presence of CNTF (Fig. 4Ab). Notably, all the Rhodopsin-expressing cells were included in the cells that expressed dominant-negative form of STAT3 as identified by HA immunostaining, and all of them were in the ONL (Fig. 4Ac). None of the cells expressing control GFP vector alone, detected by green fluorescence of GFP (Fig. 4Ad), ever expressed Rhodopsin when the explants were cultured with CNTF (Fig. 4Ae). The *crx* mRNA expression after CNTF exposure was statistically higher in the pCAG-STAT3F-electroporated P0 retinal explants than in the control pCAG-electroporated P0 retinal explants, according to the results of real-time RT-PCR analysis with normalization to *gfp* mRNA, which was the transcript from the cotransfected plasmid CAG-EGFP (1.65 ± 0.05:1.0 ± 0.09, $P < 0.05$, Fig. 4B).

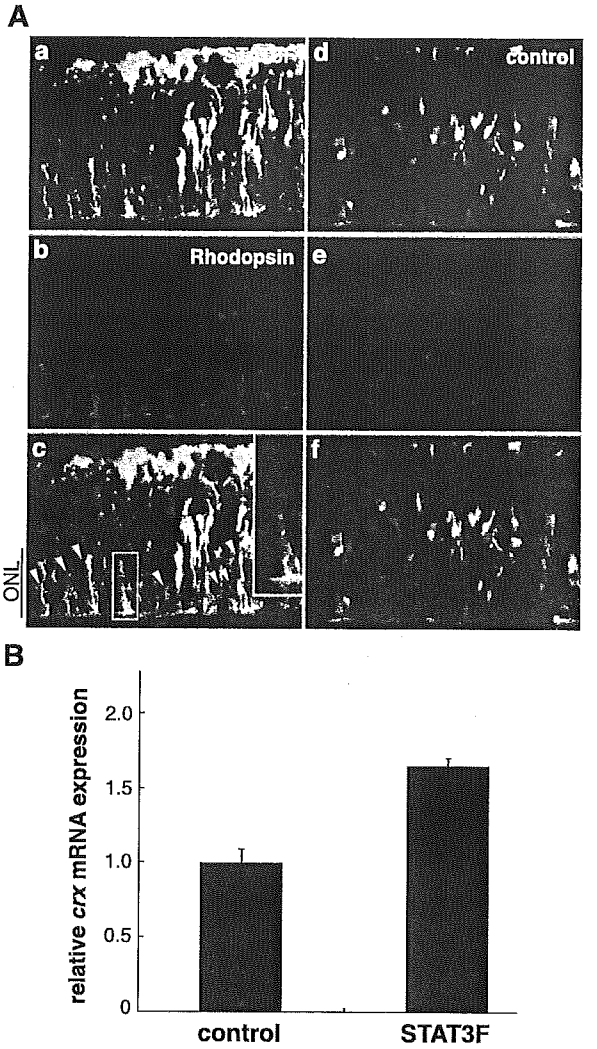

Fig. 4. Effect of CNTF in cells transfected with the dominant-negative form of STAT3 (STAT3F). (A) Wild-type retinal explants were started at P0, then electroporated and exposed to CNTF (50 ng/ml) for 7 days. STAT3F transfected cells were identified by HA immunostaining (a). Despite CNTF exposure, rhodopsin-expressing cells were observed only in the ONL (b), and they were all included in anti-HA immunopositive cells (merge, c). Inset in c: Marked area is magnified. Control vector was detected by green fluorescence protein (d), and no rhodopsin expression was seen when explants were cultured with CNTF (e, f). ONL, outer nuclear layer. (B) Real-time RT-PCR. Relative level of *crx* mRNA expression after CNTF exposure was statistically higher in cells from pCAG-STAT3F-electroporated P0 retinal explants than from control pCAG-electroporated P0 retinal explants with normalization to *gfp* mRNA, the transcript from the cotransfected plasmid CAG-EGFP (1.65 ± 0.05:1.0 ± 0.09, $P < 0.05$).

No significant effect of electroporation itself, such as cell death, abnormal retinal layer formation, or abnormal expression of differentiation markers, was observed under the present condition. Electroporated explants cultured without CNTF expressed Rhodopsin the same as untreated retinal explants (data not shown).

Thus, blockade of STAT3-mediated signaling after starting retinal explants derived from P0 mice (P0 retinal explants) was

sufficient to override the CNTF-induced inhibitory effect on Rhodopsin expression.

Furthermore, this inhibitory effect of CNTF, which was mediated by STAT3 activation, appeared to be cell-autonomous in the neural retina, since inhibition of Rhodopsin expression was overridden only in the cells in which dominant-negative form of STAT3 (STAT3F) was introduced.

Forced downregulation of STAT3 activation in the late embryonic retina was not sufficient for precocious rod photoreceptor cell differentiation

We have shown that persistent STAT3 activation by addition of CNTF in retinal explants derived from P0 mice inhibits Rhodopsin expression in vitro, and that downregulation of STAT3 activation precedes the onset of Rhodopsin expression in vivo, indicating that downregulation of STAT3 activation is required for Rhodopsin expression. We therefore investigated whether the forced downregulation of STAT3 activation in the late embryonic period induces precocious rod photoreceptor cell differentiation. If STAT3 activation is the only factor to determine the timing of rod photoreceptor cell differentiation, *crx* mRNA upregulation and Rhodopsin expression would be observed precociously in the STAT3-deficient retina. No precocious indications of Rhodopsin expression were observed, but the semiquantification analysis of *crx* mRNA expression showed some changes as described below.

Real-time RT-PCR analysis showed modest precocious upregulation of *crx* mRNA expression at E18.5 in $STAT3^{flox/-}$;α-Cre retina as compared with $STAT3^{flox/+}$ retina (1.6 ± 0.22 SE:1.0 ± 0.09 SE, $P = 0.03$, Fig. 5). The change was moderate in the mutant mice as a whole. This can be interpreted that the contribution of the STAT3 activation to inhibiting premature upregulation of *crx* mRNA is partial and some other factors may contribute in combination with STAT3 activation in vivo. In fact, we found that 25% of the individual $STAT3^{flox/-}$;α-Cre mice expressed an especially high level of *crx* mRNA, whereas the other expressed a normal (37.5%) to moderately high (37.5%) level, suggesting the presence of an alteration but with low penetrance. This suggested that there may be genetic redundancies that also affect *crx* mRNA expression.

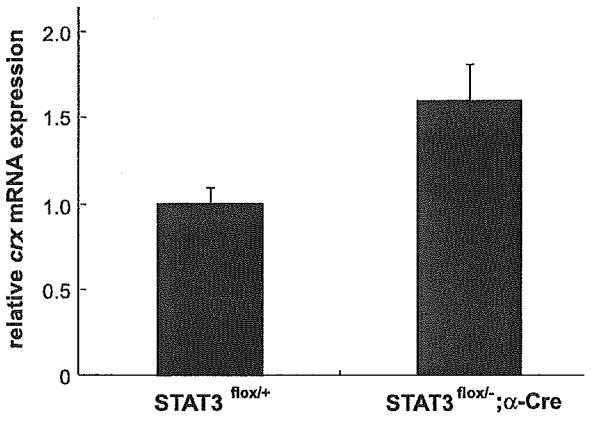

Fig. 5. Relative level of *crx* mRNA expression in STAT3-deficient retinas at E18.5. Real-time RT-PCR showed modest precocious upregulation of *crx* mRNA expression in the STAT3-deficient mice ($STAT3^{flox/-}$;α-Cre: $STAT3^{flox/+}$; 1.6 ± 0.22 SE:1.0 ± 0.09 SE, $P = 0.03$, $n = 8:6$).

There was no significant difference between $STAT3^{flox/-}$;α-Cre mice and $STAT3^{flox/+}$ mice in the numbers of the Rhodopsin-expressing cells, possibly because the time of onset of Rhodopsin expression is not determined solely by the downregulation of STAT3 activation.

We also tried to downregulate STAT3 activation in the embryonic retina in vitro by introducing STAT3F into wild-type retinal explants derived from E15 to E17 mice using electroporation. This method could rule out the possibility that the phenotypes described above are the results of indirect effects of STAT3 deficiency at some period before the birth of presumptive rod photoreceptor cells. When we examined retinal explants on the day corresponding to E18, that is, the day before initial expression of Rhodopsin in the control explants, and to P0, we found no precocious Rhodopsin positive cells in the retinal explants (data not shown), and identified Rhodopsin expression later, the same as in the unelectroporated retinal explants. This indicated that earlier blockade of STAT3 activation was insufficient to cause premature expression of Rhodopsin.

Discussion

Presumptive rod photoreceptor cells in outer half of the neural retina first appeared to be postmitotic in the late embryonic period (Cepko et al., 1996; Young, 1985) and start to express one of the terminal differentiation markers, Rhodopsin, in the early postnatal period. This interval between the final cell cycle and the onset of Rhodopsin expression is known to be several days (Morrow et al., 1998a,b). It has been postulated that both accumulation of cell intrinsic factors to promote differentiation and release from inhibitory extracellular signaling included in the embryonic retina might be important in determining the onset of Rhodopsin expression in the early postnatal period (Kirsch et al., 1998; Levine et al., 2000; Neophytou et al., 1997; Schulz-Key et al., 2002). Here we focus on the fact that CNTF that is present in the embryonic retina and downregulated in the postnatal retina inhibits Rhodopsin expression (Ezzeddine et al., 1997; Kirsch et al., 1998; Levine et al., 2000; Neophytou et al., 1997; Schulz-Key et al., 2002). We demonstrate that STAT3 activation mediates this inhibition, via one of the photoreceptor cell-specific gene activator, *crx*. Furthermore, we demonstrate that the negative correlation of Rhodopsin expression and STAT3 activation in perinatal retina and downregulation of STAT3 activation are required, although not sufficient, for presumptive rod photoreceptor cells to differentiate into rod photoreceptor cells.

CNTF downregulates expression of crx and Rhodopsin via STAT3 activation in P0 retinal explants

To analyze the mechanism of the CNTF-induced inhibition of Rhodopsin expression, we utilized the organ culture system of mouse neural retina started at P0, since this system maintains the microenvironmental condition surrounding the presumptive rod photoreceptor cells similar to that in vivo, in terms of cell density, cell distribution, and temporal expression profiles of various cell-type-specific markers of the retinal cells (Tomita et al., 1996), and it also allowed us to introduce exogenous genes of interest easily. We confirmed that CNTF exposure induces the inhibition of Rhodopsin expression while sustaining the competence for rod photoreceptor cells in P0 retinal explants.

In the present study, we showed that CNTF also downregulated homeobox gene *crx* dramatically. *crx* is one of the upstream transcription activators of *rhodopsin,* and rapid upregulation of *crx* expression is well correlated with the rapid increase in Rhodopsin expression as well as the expression of a series of photoreceptor-specific genes during normal retinal development (Chen et al., 1997; Furukawa et al., 1997, 1999, 2002; Livesey et al., 2000). Besides, expression of photoreceptor-specific genes including *rhodopsin* is greatly reduced in Crx knock-out mice (Furukawa et al., 1999). Thus, downregulation of the expression of photoreceptor-specific genes including *rhodopsin* by CNTF may occur through *crx* repression.

Then, which signal transduction pathway downstream from CNTF inhibited the expression of *crx* and Rhodopsin? CNTF is one of cytokines that activates gp130 receptor together with leukemia inhibitory factor (LIF) receptor β. They in turn recruit signal transducing molecules, such as STAT3 and SHP2, through which CNTF-induced cytokine signaling diverges into multiple downstream pathways that regulate cell growth, differentiation, survival, and so on (Hirano et al., 1997; Ohtani et al., 2000). Although both the STAT3- and SHP2-mediated pathways may be potentially activated in onbl/ONL cells following exposure to CNTF, expression of *crx* and Rhodopsin was only inhibited in the cells in which STAT3 had been activated. In addition, when CNTF exposure was discontinued and STAT3 activation was downregulated, Rhodopsin expression resumed, raising the possibility that STAT3 activation may be the cause of inhibition of Rhodopsin expression.

To test this possibility, we attempted to separate signaling pathways, which are supposed to be activated by CNTF, by preparing mutant P0 retinal explants from STAT3 conditional knock-out mice or gp130 mutant mice that are unable to activate SHP2 and investigated the inhibitory effect of CNTF in each culture. Our results demonstrated that STAT3 activation, but not SHP2 activation, is required for the CNTF-induced inhibitory effect on expression of *crx* and Rhodopsin in the ONL of P0 retinal explants.

It is still possible that earlier disruption of STAT3 gene might indirectly contribute to the lack of inhibitory effect of CNTF on expression of *crx* and Rhodopsin in the P0 retinal explants, since α-Cre-mediated gene disruption of the STAT3 locus occurs in the mid-embryonic period in $STAT3^{flox/-}$;α-Cre mice. To assess this possibility, we introduced dominant-negative form of STAT3, STAT3F, into P0 retinal explants of wild-type postnatal neural retina to disrupt functional STAT3 only after starting P0 retinal explants. For this purpose, we developed electroporation system allowing direct introduction of exogenous genes of interest into cells regardless of their stage of their cell cycle, in contrast to the method of retroviral infection (Tomita et al., 1996). We are able to transfect any gene into the organ culture including both postmitotic cells as well as mitotic cells by this method (data not shown). Moreover, the scattered population of transfected cells is appropriate to examine the cell-autonomous effect after gene introduction. No significant harmful effect of electroporation itself was observed and electroporated explant cells survived well for 7–10 days, in the same way as non-electroporated retinal explant cells. Expression of the gene introduced was sustained for at least 10 days under the conditions in this study. This demonstrates that blockade of STAT3 activation in ONL cells only after starting retinal explants derived from P0 mice is sufficient to override the CNTF-induced inhibition of expression of *crx* and Rhodopsin in a cell-autonomous manner. Although STAT3F expressing cells identified by anti-HA-immunostaining were widely distributed throughout all retinal layers, Rhodopsin expression occurred only in the ONL, suggesting that the potential to differentiate into rod photoreceptor cells is already restricted to the cells in the ONL.

Thus, it is now clear that STAT3 activation, induced by CNTF, is responsible for inhibition of expression of *crx* and Rhodopsin in the retinal explants derived from P0 mice (P0 retinal explants).

Molecular mechanisms of CNTF-induced inhibition of expression of crx and Rhodopsin

Knowing that STAT3 activation is the main cause of CNTF-induced downregulation of expression of Rhodopsin and its upstream activator, *crx* expression, several molecular mechanisms can be considered to explain the STAT3-mediated inhibitory effect on their expression. *crx* is one of the transcription activators of *rhodopsin* and is suggested to elevate expression level through the positive feedback mechanism (Furukawa et al., 2002) as discussed below. Thus, it is more important to identify the mechanism of *crx* repression to explain the mechanisms of inhibition of Rhodopsin expression.

Active STAT3 may bind to the upstream cis element of the *crx* gene near the sequence necessary for its activation to interfere the efficient approach and/or function of positive regulators competitively. This type of repression mechanism has been proposed in olfactory receptor neurons, in which the LIF/gp130 signal plays critical roles in maturation (Moon et al., 2002). Moon et al. showed that active STAT3 directly binds in the proximal resion of the promoter of *olfactory marker protein* gene, near the binding sites of the tissue-specific transcription activators, and negatively regulated the transcription. Since there is indeed a STAT3 binding consensus sequence upstream of the *crx* transcription initiation site, an excess of active STAT3 might affect binding of Crx or some other specific activators in a similar mechanism.

Another possibility is that active STAT3 sequesters cofactors, such as CBP/p300, that are required to induce *crx* gene expression. Assuming that the amounts of these cofactors in a cell are limited, they may be recruited competitively among various kinds of transcription factors. It is known that activation of bHLH transcription factors limit the level of common cofactors, CBP/p300, and inhibit STAT3 activation in neuronal cells (Sun et al., 2001). If CBP/p300 may be required for Crx (Yanagi et al., 2000) and bHLH gene products that may activate *crx* and/or *rhodopsin* genes (Ahmad, 1995), lack of CBP/p300, after excess of active STAT3 recruited CBP/p300 dominantly, might affect *crx* and/or *rhodopsin* gene expression.

It must be considered that there is a possibility that CNTF downregulates other transcription activators that upregulate Rhodopsin expression, whether functioning with Crx or not (Kimura et al., 2000; Mitton et al., 2000). For example, the transcription factor, neural retina leucine zipper (Nrl), has been shown to be one of the molecules essential for expression of *rhodopsin* and several other rod photoreceptor-specific genes based on the analyses of Nrl knock-out mice (Mears et al., 2001). There are still possibilities that STAT3 represses *rhodopsin* promoter directly or indirectly other than through repression of *crx*.

The effect of STAT3 on transcription of *crx* and *rhodopsin* may be regulated at multiple levels.

What determines the timing of the differentiation of postmitotic retinal cells in the ONL into rod photoreceptor cells?

As discussed above, presumptive rod photoreceptor cells in the ONL that exited cell cycle in the late embryonic period are kept undifferentiated until they rapidly upregulate *crx* expression and start to express the terminal differentiation marker Rhodopsin in the early postnatal period. How is this process precisely controlled? Obviously, both positive and negative factors may be involved (Kageyama and Nakanishi, 1997). Regarding negative factors, we propose STAT3 activation by CNTF that prevents presumptive rod photoreceptor cells from differentiation, based on the negative correlation between STAT3 activation and Rhodopsin expression during retinal development in vivo, and the results of persistent STAT3 activation in vitro; STAT3 was highly activated in presumptive rod photoreceptor cells at E18.5, and was rapidly inactivated to below the level of detection at P0, which corresponded to the onset of rapid upregulation of *crx* and Rhodopsin expression (Fig. 6Aa). If persistent STAT3 activation occurs in presumptive rod photoreceptor cells in P0 retinal explants, neither *crx* nor Rhodopsin can be upregulated (Fig. 6Ab). Active STAT3 allows the presumptive rod photoreceptor cells to retain their competence to differentiate into rod photoreceptor cells, and differentiation can be restarted as long as the inhibitory extrinsic cue is eliminated (Figs. 1Ab, d, m, n, and 4b), which is consistent with the estimated function in vivo.

Then, is downregulation of STAT3 activation sufficient to trigger Rhodopsin expression? To answer this question, we investigated whether conditional disruption of STAT3 in the late embryonic period leads to precocious differentiation of rod photoreceptor cells. If STAT3 activation were the only factor to determine the time of onset, Rhodopsin expression would start before P0 in STAT3-deficient mice. However, that did not happen at significant level. But semiquantitative analysis by real-time RT-PCR showed that 25% of the individual mutant retinas exhibited precocious upregulation of *crx* mRNA, suggesting that downregulation of STAT3 activation has at least some roles in determining the time of onset of rod photoreceptor cell differentiation. This change was moderate in the mutants as a whole, but obvious in 25% of the individual mutant embryonic retinas. The low penetrant change often indicates genetic redundancies; therefore, some other factors besides downregulation of STAT3 activation may be necessary to determine the time of onset of upregulation of *crx* mRNA. This is why we consider that downregulation of STAT3 activation might contribute to determin-

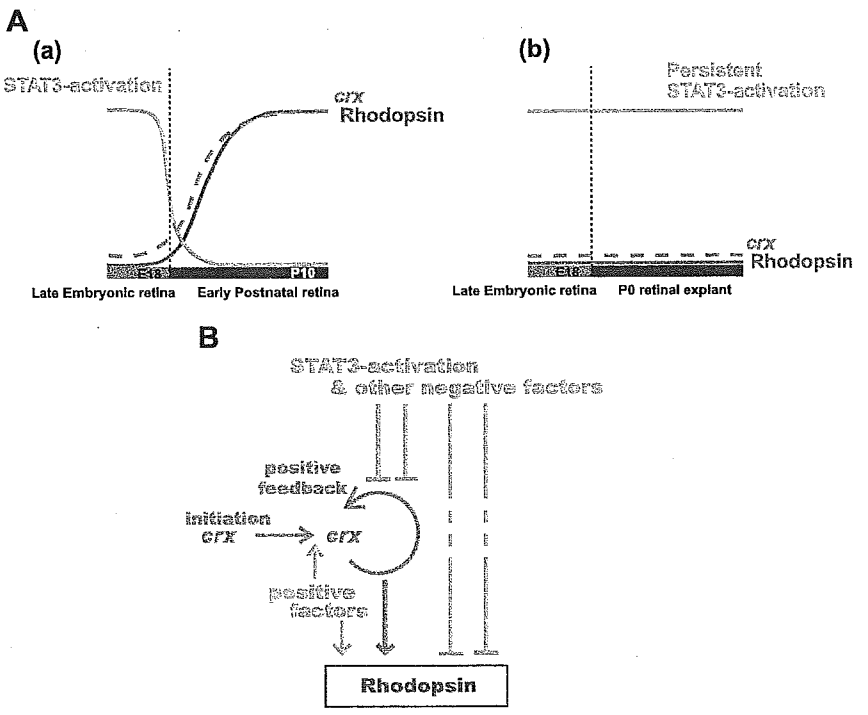

Fig. 6. (A) Molecular mechanisms regulating rod photoreceptor cell differentiation in perinatal retina. Rod photoreceptor cells differentiate in the outer layer of the neural retina. STAT3 is highly activated in this layer of the late embryonic retina in vivo, but its activation is rapidly downregulated in the early postnatal retina. This allows upregulation of *crx* transcription, which in turn contributes to upregulation of expression of Rhodopsin, one of the terminal differentiation markers, in the early postnatal retina (a). Persistent STAT3 activation in this layer of P0 retinal explants prevents upregulation of *crx* transcription and Rhodopsin expression in a cell-autonomous manner (b). (B) A model for STAT3 activation as one of the potential negative regulators of *crx* and Rhodopsin expression. We hypothesize that STAT3 activation contributes as one of the potential negative regulators of *crx* and Rhodopsin expression based on our results of STAT3-deficient mice and stage-specific disruption of STAT3 activation after introducing the dominant-negative STAT3 (STAT3F). We propose a model in which STAT3 activation inhibits a high level of *crx* expression that is upregulated possibly via a positive feedback mechanism. Several other factors, including positive and/or negative factors, would contribute together. STAT3 activation inhibits Rhodopsin expression mainly through inhibition of a high level of *crx* expression and possibly through other pathways that are regulated by positive and/or negative factors. Thus, downregulation of STAT3 activation might contribute partially, although not definitively, to determining the time of onset of Rhodopsin expression in presumptive rod photoreceptor cells.

ing the time of onset of rod photoreceptor cell differentiation in the presumptive rod photoreceptor cells, although it is not a major contribution. This kind of low penetrant phenotype is also observed in a certain gene disrupted mice, such as Ring 1A-deficient mice that have an only low penetrant homeotic alteration in the axial skeleton associated with minor alterations of Hox gene expression (del Mar Lorente et al., 2000). Since Ring 1A functions only as one of the members of transcriptional repressors that negatively regulate Hox gene expression, other members of transcriptional repressors, such as Ring 1B, would compensate the function in Ring 1A-deficient mice.

Knowing that STAT3 activation is not absolutely crucial for the suppression of Rhodopsin expression in the embryonic period, we propose a possible influence of STAT3 activation on *crx* expression. It has been suggested that transcriptional regulation of *crx* is divided into two steps (Furukawa et al., 2002). In the first step, *crx* is initially expressed at a low level in the late embryonic period, and in the second step, rapid upregulation occurs possibly mediated via a positive feedback mechanism by Crx itself together with unknown factors (Furukawa et al., 2002). Based on our observations, the first step of this model begins despite continuous STAT3 activation, while the second step initiated in the early postnatal period after STAT3 activation has declined. Here we show that a high level of *crx* expression is inhibited by STAT3 activation induced by addition of CNTF in the P0 retinal explants, and this may be attributable to the inhibition of the second step (Fig. 6B). Taken together, the attractive model involves a low level of expression that is insensitive to the negative effect of STAT3 activation in the late embryonic period and a high level of expression that is sensitive to the negative effect of STAT3 activation in the early postnatal period. Lack of precocious expression of Rhodopsin even in the absence of STAT3 activation in the late embryonic period instead supports the notion that a combination of Crx and other factors, as yet unidentified, is required for the high level of *crx* expression that allows Rhodopsin expression in postmitotic retinal cells in the ONL. In addition, positive factors promoting Rhodopsin expression other than Crx and/or the suppression of certain negative factors other than the STAT3 activation would be necessary for the Rhodopsin expression and/or rod photoreceptor cell differentiation.

In conclusion, we propose here one of the potential regulatory mechanisms for rod photoreceptor cell differentiation in terms of expression of *crx* and Rhodopsin in the perinatal period. Downregulation of STAT3 activation is required in the postnatal period for proper rod photoreceptor cell differentiation. Furthermore, it is conceivable that downregulation of STAT3 activation contributes as one of the factors to determining the time of onset of rod photoreceptor cell differentiation, although further analyses are required to clarify other factors.

Experimental methods

Neural retinal explant culture

Retinal explant culture was performed using P0 mouse neural retina based on the protocol described by Tomita et al. (1996). Briefly, eyes were enucleated and neural retinas were isolated and placed on a Millicell chamber filter (Millipore: pore size: 0.4 μm) with the ganglion cell layer facing up. The chamber was then placed in a 6-well culture plate, containing 50% MEM (GIBCO), 25% HBSS (GIBCO), 25% horse serum (Thermo Trace), 200 mM L-glutamine, and 6.75 mg/ml D-glucose. Explants were incubated at 34°C in 5% CO_2. Medium was changed every 1–2 days.

A 10 μg/ml stock solution of recombinant rat CNTF (R&D) in MEM was maintained at −20°C. Once thawed, it was maintained at 4°C and used within 3 days. CNTF was used in concentrations of 50–100 ng/ml in this system, just enough to completely inhibit Rhodopsin expression in the ONL of P0 retinal explants, without causing any obvious changes in the three-layered structure of the retina, in the morphology of any of the cell types, or in expressions of molecular markers of cell types other than rod photoreceptor cells. These concentrations are somewhat higher than those used in previous studies (Ezzeddine et al., 1997; Kirsch et al., 1998; Schulz-Key et al., 2002), in part because the medium contained a relatively large amount of horse serum that may include antagonizing activity to CNTF, or because the membrane inserted between the explants and the medium affected our culture system.

Animals

ICR and C57B/6 mice were purchased from Clea Japan, INC. and the Charles River Laboratory.

STAT3 ^{flox} mice and STAT3$^{+/-}$ mice were generated by Dr. Akira's Lab (Sano et al., 1999; Takeda et al., 1997), and gp130^{F759} knock-in mice by Dr. Hirano's Lab (Ohtani et al., 2000). α-Cre transgenic mice, which express Cre-recombinase only in the retina, were generously provided by Dr. Gruss (Marquardt et al., 2001). The mice were used in conjunction with genotyping. CAG-CAT-EGFP transgenic mice, used to show the expression of Cre-recombinase, were kindly provided by Dr. Miyazaki (Kawamoto et al., 2000).

In the experiments on mutant mice, P0 retinal explant from one eye was exposed to CNTF and P0 retinal explants from the other eye was not exposed to CNTF to equalize the basal developmental stage.

Immunohistochemistry

Cryosections (12–14 μm) of retinal explants were fixed with 4% paraformaldehyde and prepared as described elsewhere (Tomita et al., 1996). Cryosections of E18.5 and P0 eyes (12 μm) were prepared by perfusing mice with 4% paraformaldehyde, enucleated, and post-fixed in 4% paraformaldehyde. Sections were first incubated with 0.1% Triton, 10% goat serum in PBS, and then at 4°C with primary antibodies to retinal cell-specific markers, that is, rabbit anti-Rhodopsin (1:2000 LSL), mouse anti-glutamine synthetase (1:400 Molecular Probe), mouse anti-HPC1 (1:600 Sigma), and mouse anti-PKCα (1:50 Molecular Probe), diluted in 0.1% Triton and 2% goat serum. Sections were then incubated with the secondary antibody, Alexa 568-conjugated goat anti-rabbit, or Alexa 488-conjugated goat anti-mouse IgG (1:500, Molecular Probe), respectively. For immunostaining of rabbit anti-phosphoSTAT3 (1:50 Cell Signaling) and rat anti-HA (1:500, Roche Diagnostics GmbH), sections were pre-incubated at 100°C for 5 min with tissue retrieval solution (TRS, Sigma #1699) and then placed on ice for 20 min. Next, they were incubated in 1% H_2O_2, in blocking agent, and then at 4°C overnight, with primary antibody diluted in blocking agent with 0.3% or 0.1% Triton, respectively. The sections were incubated with biotin-conjugated donkey anti-rabbit IgG (1:500 Chemicon) or biotin-conjugated goat anti-rat IgG (1:500, Vector), then with prepared avidin-biotin-peroxidase complex (Vector). Finally,

immunoreactions were detected with a tyramide signal amplification (TSA) fluorescein system (Perkin Elmer Life Science). Nuclei were stained with the nuclear dye bisbenzimide 1:1000 from a stock solution of 10 mg/ml Hoechst 33258 (Sigma). GFP fluorescence disappeared after TRS treatment. For double immunostaining, all processes were performed sequentially. To strip away the primary antibody, sections were incubated with 200 mM glycine (pH 2.2). The double immunostained sections were examined with a laser scanning confocal microscope (LSM510, Carl Zeiss).

Real-time RT-PCR

Total RNA was extracted from retina, and cDNAs were synthesized after RNase-free DNase (Invitrogen) treatment. Real-time PCR was performed using an ABI PRISM 7700, with SYBR green (Molecular Probe). The primers for *crx* detection have been described by Furukawa et al. (1999). The results are presented as ratios of mRNA expression normalized to an inner control gene: *β-actin* or *gfp* mRNA in electroporated cells.

Immunoblot analysis

Retinal cells from the outer layer were collected by cutting the neural retina horizontally, as described by Schulz-Key et al. (2002) with minor modification. Briefly, neural retinal explants and neural retinas were flat-mounted and cryosections were made at a 60-μm thickness from the ONL/onbl side. The extracts were electrophoretically transferred to membranes and incubated in rabbit anti-STAT3 (1:1000, Cell Signaling) or rabbit anti-phosphoSTAT3 (1:1000, Cell Signaling), with mouse anti-α-tubulin (1:2000, Sigma) to equalize the amount of protein in each sample, then with both horseradish peroxidase-conjugated anti-rabbit IgG and anti-mouse IgG. The specific proteins were detected with an ECL system (Pharmacia-Amersham).

Electroporation

DNA, 5 μg/μl in PBS(−), was loaded on the top of agarose gel placed on a plate-type electrode. After a retinal explant on the membrane had been placed on the DNA, a disk type electrode was used to apply electric pulses (20 V, 50 ms, 6 times) with the electroporator (CUY21 NEPPA GENE), without contacting the tissue. The retinal explant was then immediately replaced in the medium and incubated as described above. An expression vector carrying a cDNA encoding a dominant-negative form of STAT3F (Minami et al., 1996; Nakajima et al., 1996) under control of the CAG promoter (Niwa et al., 1991), pCAG-STAT3F, was cotransfected with pCAG-EGFP (an expression vector containing the enhanced green fluorescent protein [EGFP]) (10:1). Empty transfection vector, pCAG, with pCAG-EGFP was electroporated as a control.

In situ hybridization

In situ hybridization was performed on 12- to 14-μm-thick cryosections. The probe for *crx* (a generous gift from Dr. Furukawa) (Furukawa et al., 1997) was full-length and detected with a digoxigenin labeling system. To compare expression levels, these processes were simultaneously performed in parallel under the same conditions on the same glass.

Acknowledgments

We appreciate Dr. Peter Gruss for generously providing the α-Cre transgenic mice, Dr. Takahisa Furukawa for the *crx* cDNA, Dr. Jun-ichi Miyazaki for the CAG-CAT-EGFP transgenic mice, and Dr. Hitoshi Niwa for the plasmid CAG. We also thank Hironori Kawahara for preparing the illustrations. This work was supported by grants from the Ministry of Education, Science and Culture of Japan to H.O. and National Grant-in-Aid for the Establishment of High-Tech Research Center in a Private University.

References

Ahmad, I., 1995. Mash-1 is expressed during ROD photoreceptor differentiation and binds an E-box, E(opsin)-1 in the rat opsin gene. Brain Res., Dev. Brain Res. 90, 184–189.

Akira, S., 1999. Functional roles of STAT family proteins: lessons from knockout mice. Stem Cells 17, 138–146.

Alessi, D.R., Cuenda, A., Cohen, P., Dudley, D.T., Saltiel, A.R., 1995. PD 098059 is a specific inhibitor of the activation of mitogen-activated protein kinase kinase in vitro and in vivo. J. Biol. Chem. 270, 27489–27494.

Altshuler, D., Cepko, C., 1992. A temporally regulated, diffusible activity is required for rod photoreceptor development in vitro. Development 114, 947–957.

Altshuler, D., Lo Turco, J.J., Rush, J., Cepko, C., 1993. Taurine promotes the differentiation of a vertebrate retinal cell type in vitro. Development 119, 1317–1328.

Baumer, N., Marquardt, T., Stoykova, A., Ashery-Padan, R., Chowdhury, K., Gruss, P., 2002. Pax6 is required for establishing naso-temporal and dorsal characteristics of the optic vesicle. Development 129, 4535–4545.

Belliveau, M.J., Young, T.L., Cepko, C.L., 2000. Late retinal progenitor cells show intrinsic limitations in the production of cell types and the kinetics of opsin synthesis. J. Neurosci. 20, 2247–2254.

Cepko, C.L., Austin, C.P., Yang, X., Alexiades, M., Ezzeddine, D., 1996. Cell fate determination in the vertebrate retina. Proc. Natl. Acad. Sci. U. S. A. 93, 589–595.

Chen, S., Wang, Q.L., Nie, Z., Sun, H., Lennon, G., Copeland, N.G., Gilbert, D.J., Jenkins, N.A., Zack, D.J., 1997. Crx, a novel Otx-like paired-homeodomain protein, binds to and transactivates photoreceptor cell-specific genes. Neuron 19, 1017–1030.

del Mar Lorente, M., Marcos-Gutiérrez, C., Pérez, C., Schoorlemmer, J., Ramírez, A., Magin, T., Vidal, M., 2000. Loss- and gain-of-function mutations show a Polycomb group function for Ring1A in mice. Development 127, 5093–5100.

Edlund, T., Jessell, T.M., 1999. Progression from extrinsic to intrinsic signaling in cell fate specification: a view from the nervous system. Cell 96, 211–224.

Ezzeddine, Z.D., Yang, X., DeChiara, T., Yancopoulos, G., Cepko, C.L., 1997. Postmitotic cells fated to become rod photoreceptors can be respecified by CNTF treatment of the retina. Development 124, 1055–1067.

Furukawa, T., Morrow, E.M., Cepko, C.L., 1997. Crx, a novel otx-like homeobox gene, shows photoreceptor-specific expression and regulates photoreceptor differentiation. Cell 91, 531–541.

Furukawa, T., Morrow, E.M., Li, T., Davis, F.C., Cepko, C.L., 1999. Retinopathy and attenuated circadian entrainment in Crx-deficient mice. Nat. Genet. 23, 466–470.

Furukawa, A., Koike, C., Lippincott, P., Cepko, C.L., Furukawa, T., 2002. The mouse Crx 5′-upstream transgene sequence directs cell-specific and developmentally regulated expression in retinal photoreceptor cells. J. Neurosci. 22, 1640–1647.

Harris, W.A., 1997. Cellular diversification in the vertebrate retina. Curr. Opin. Genet. Dev. 7, 651–658.

Hirano, T., Nakajima, K., Hibi, M., 1997. Signaling mechanisms through gp130: a model of the cytokine system. Cytokine Growth Factor Rev. 8, 241–252.

Kageyama, R., Nakanishi, S., 1997. Helix-loop-helix factors in growth and differentiation of the vertebrate nervous system. Curr. Opin. Genet. Dev. 7, 659–665.

Kawamoto, S., Niwa, H., Tashiro, F., Sano, S., Kondoh, G., Takeda, J., Tabayashi, K., Miyazaki, J., 2000. A novel reporter mouse strain that expresses enhanced green fluorescent protein upon Cre-mediated recombination. FEBS Lett. 470, 263–268.

Kelley, M.W., Turner, J.K., Reh, T.A., 1994. Retinoic acid promotes differentiation of photoreceptors in vitro. Development 120, 2091–2102.

Kimura, A., Singh, D., Wawrousek, E.F., Kikuchi, M., Nakamura, M., Shinohara, T., 2000. Both PCE-1/RX and OTX/CRX interactions are necessary for photoreceptor-specific gene expression. J. Biol. Chem. 275, 1152–1160.

Kirsch, M., Lee, M.Y., Meyer, V., Wiese, A., Hofmann, H.D., 1997. Evidence for multiple, local functions of ciliary neurotrophic factor (CNTF) in retinal development: expression of CNTF and its receptors and in vitro effects on target cells. J. Neurochem. 68, 979–990.

Kirsch, M., Schulz-Key, S., Wiese, A., Fuhrmann, S., Hofmann, H., 1998. Ciliary neurotrophic factor blocks rod photoreceptor differentiation from postmitotic precursor cells in vitro. Cell Tissue Res. 291, 207–216.

Levine, E.M., Fuhrmann, S., Reh, T.A., 2000. Soluble factors and the development of rod photoreceptors. Cell. Mol. Life Sci. 57, 224–234.

Lillien, L., 1995. Changes in retinal cell fate induced by overexpression of EGF receptor. Nature 377, 158–162.

Livesey, F.J., Cepko, C.L., 2001. Vertebrate neural cell-fate determination: lessons from the retina. Nat. Rev., Neurosci. 2, 109–118.

Livesey, F.J., Furukawa, T., Steffen, M.A., Church, G.M., Cepko, C.L., 2000. Microarray analysis of the transcriptional network controlled by the photoreceptor homeobox gene Crx. Curr. Biol. 10, 301–310.

Marquardt, T., Ashery-Padan, R., Andrejewski, N., Scardigli, R., Guillemot, F., Gruss, P., 2001. Pax6 is required for the multipotent state of retinal progenitor cells. Cell 105, 43–55.

Mears, A.J., Kondo, M., Swain, P.K., Takada, Y., Bush, R.A., Saunders, T.L., Sieving, P.A., Swaroop, A., 2001. Nrl is required for rod photoreceptor development. Nat. Genet. 29, 447–452.

Minami, M., Inoue, M., Wei, S., Takeda, K., Matsumoto, M., Kishimoto, T., Akira, S., 1996. STAT3 activation is a critical step in gp130-mediated terminal differentiation and growth arrest of a myeloid cell line. Proc. Natl. Acad. Sci. U. S. A. 93, 3963–3966.

Mitton, K.P., Swain, P.K., Chen, S., Xu, S., Zack, D.J., Swaroop, A., 2000. The leucine zipper of NRL interacts with the CRX homeodomain. A possible mechanism of transcriptional synergy in rhodopsin regulation. J. Biol. Chem. 275, 29794–29799.

Moon, C., Yoo, J.Y., Matarazzo, V., Sung, Y.K., Kim, E.J., Ronnett, G.V., 2002. Leukemia inhibitory factor inhibits neuronal terminal differentiation through STAT3 activation. Proc. Natl. Acad. Sci. U. S. A. 99, 9015–9020.

Morrow, E.M., Belliveau, M.J., Cepko, C.L., 1998a. Two phases of rod photoreceptor differentiation during rat retinal development. J. Neurosci. 18, 3738–3748.

Morrow, E.M., Furukawa, T., Cepko, C.L., 1998b. Vertebrate photoreceptor cell development and disease. Trends Cell Biol. 8, 353–358.

Nakajima, K., Yamanaka, Y., Nakae, K., Kojima, H., Ichiba, M., Kiuchi, N., Kitaoka, T., Fukada, T., Hibi, M., Hirano, T., 1996. A central role for Stat3 in IL-6-induced regulation of growth and differentiation in M1 leukemia cells. EMBO J. 15, 3651–3658.

Neophytou, C., Vernallis, A.B., Smith, A., Raff, M.C., 1997. Muller-cell-derived leukaemia inhibitory factor arrests rod photoreceptor differentiation at a postmitotic pre-rod stage of development. Development 124, 2345–2354.

Niwa, H., Yamamura, K., Miyazaki, J., 1991. Efficient selection for high-expression transfectants with a novel eukaryotic vector. Gene 108, 193–199.

Ohtani, T., Ishihara, K., Atsumi, T., Nishida, K., Kaneko, Y., Miyata, T., Itoh, S., Narimatsu, M., Maeda, H., Fukada, T., et al., 2000. Dissection of signaling cascades through gp130 in vivo: reciprocal roles for STAT3- and SHP2-mediated signals in immune responses. Immunity 12, 95–105.

Sano, S., Itami, S., Takeda, K., Tarutani, M., Yamaguchi, Y., Miura, H., Yoshikawa, K., Akira, S., Takeda, J., 1999. Keratinocyte-specific ablation of Stat3 exhibits impaired skin remodeling, but does not affect skin morphogenesis. EMBO J. 18, 4657–4668.

Schulz-Key, S., Hofmann, H.D., Beisenherz-Huss, C., Barbisch, C., Kirsch, M., 2002. Ciliary neurotrophic factor as a transient negative regulator of rod development in rat retina. Invest. Ophthalmol. Visual Sci. 43, 3099–3108.

Sun, Y., Nadal-Vicens, M., Misono, S., Lin, M.Z., Zubiaga, A., Hua, X., Fan, G., Greenberg, M.E., 2001. Neurogenin promotes neurogenesis and inhibits glial differentiation by independent mechanisms. Cell 104, 365–376.

Takeda, K., Akira, S., 2000. STAT family of transcription factors in cytokine-mediated biological responses. Cytokine Growth Factor Rev. 11, 199–207.

Takeda, K., Noguchi, K., Shi, W., Tanaka, T., Matsumoto, M., Yoshida, N., Kishimoto, T., Akira, S., 1997. Targeted disruption of the mouse Stat3 gene leads to early embryonic lethality. Proc. Natl. Acad. Sci. U. S. A. 94, 3801–3804.

Tomita, K., Ishibashi, M., Nakahara, K., Ang, S.L., Nakanishi, S., Guillemot, F., Kageyama, R., 1996. Mammalian hairy and enhancer of split homolog 1 regulates differentiation of retinal neurons and is essential for eye morphogenesis. Neuron 16, 723–734.

Watanabe, T., Raff, M.C., 1990. Rod photoreceptor development in vitro: intrinsic properties of proliferating neuroepithelial cells change as development proceeds in the rat retina. Neuron 4, 461–467.

Yanagi, Y., Masuhiro, Y., Mori, M., Yanagisawa, J., Kato, S., 2000. p300/CBP acts as a coactivator of the cone-rod homeobox transcription factor. Biochem. Biophys. Res. Commun. 269, 410–414.

Young, R.W., 1985. Cell differentiation in the retina of the mouse. Anat. Rec. 212, 199–205.

Journal of Neurochemistry, 2004, **90**, 142–154 doi:10.1111/j.1471-4159.2004.02470.x

Mapping spatio-temporal activation of Notch signaling during neurogenesis and gliogenesis in the developing mouse brain

Akinori Tokunaga,*,†,‡ Jun Kohyama,* Tetsu Yoshida,* Keiko Nakao,*,† Kazunobu Sawamoto*,† and Hideyuki Okano*,†

**Department of Physiology, Keio University School of Medicine, Tokyo, Japan*

†Core Research for Evolutional Science and Technology (CREST), Japan Science and Technology Agency, Saitama, Japan

‡Osaka University Graduate School of Medicine, Suita, Osaka, Japan

Abstract

Notch1 plays various important roles including the maintenance of the stem cell state as well as the promotion of glial fates in mammalian CNS development. However, because of the very low amount of the activated form of Notch1 present *in vivo*, its precise activation pattern has remained unknown. In this study, we mapped the active state of this signaling pathway *in situ* in the developing mouse brain using a specific antibody that recognizes the processed form of the intracellular domain of Notch1 cleaved by presenilin/γ-secretase activity. By using this antibody, active state of Notch1 came to be detectable with a higher sensitivity than using conventional antibody against Notch1. We found that activated Notch1 was mainly detected in the nuclei of a subpopulation of radial glial cells, the majority of proliferating precursor cells in the ventricular zone (VZ). However, Notch1 activation was not detected in neuronal precursor cells positive for neuronal basic helix-loop-helix proteins or in differentiating neurons in the embryonic forebrain. Interestingly, we found that Notch1 was transiently activated in the astrocytic lineage during perinatal CNS development. Taken together, the present method has enabled us to determine the timing, gradients, and boundaries of the activation of Notch signaling.

Keywords: activated Notch1, gliogenesis, Mash1, neurogenesis, neurogenin2, radial glia.

J. Neurochem. (2004) **90**, 142–154.

During mammalian CNS development, neurons and glia are generated from common neural progenitor cells [multipotent neural stem cells (NSCs)] (Qian *et al.* 2000; Anderson 2001; Okano 2002; Sun *et al.* 2003). In this process, Notch signaling regulates the differentiation state of NSCs in a context-dependent manner (Beatus and Lendahl 1998; Artavanis-Tsakonas *et al.* 1999; Gaiano and Fishell 2002). When Notch receptors (Notch1–4 in vertebrates) (Weinmaster *et al.* 1991) are activated by their ligands, encoded by the Delta/Serrate/lag-2 (DSL) genes, the intracellular domain (ICD) of Notch is cleaved by presenilin/γ-secretase (Selkoe and Kopan 2003). The Notch1-ICD (N1-ICD) then translocates into the nucleus to form a complex with CSL (CBF1/RBP-J in mammals) (Kato *et al.* 1997) and activates the transcription of the basic helix-loop-helix (bHLH) genes *Hes1* and *Hes5*, which act as downstream effectors of Notch (de la Pompa *et al.* 1997; Kageyama and Nakanishi 1997; Nakamura *et al.* 2000; Ross *et al.* 2003). Hes1 and Hes5 repress the expression of proneural bHLH genes such as *Mash1* (Ishibashi *et al.* 1995). The proneural bHLH factors (e.g. Mash1, Neurogenin1 and Neurogenin2) are likely to be involved in the transition from NSC to progenitor cell (Torii *et al.* 1999; Nieto *et al.* 2001; Sun *et al.* 2001). Thus, the activation of Notch signaling inhibits neuronal commitment in the cells that receive it.

Received November 13, 2003; revised manuscript received January 10, 2004; accepted February 20, 2004.

Address correspondence and reprint requests to H. Okano, Department of Physiology, Keio University School of Medicine, 35 Shinanomachi, Shinjuku-ku, Tokyo 160-8582, Japan.
E-mail: hidokano@sc.itc.keio.ac.jp

Abbreviations used: bHLH, basic helix-loop-helix; BLBP, brain lipid binding protein; DMEM, Dulbecco's modified Eagle's medium; DSL, Delta/Serrate/lag-2; GE, ganglionic eminence; GFAP, glial fibrillary acidic protein; GS, glutamine synthetase; ICD, intracellular domain; IR, immunoreactivity; LGE, lateral ganglionic eminence; N1-ICD, Notch1-ICD; NSC, neural stem cell; PBS, phosphate buffered saline; PCNA, proliferating cell nuclear antigen; PFA, paraformaldehyde; SDS–PAGE, sodium dodecyl sulfate–polyacrylamide gel electrophoresis; VZ, ventricular zone.

Notch1-mediated signal pathways play crucial roles in mammalian CNS development, including in maintenance of a neural stem cell (progenitor) state, inhibition of neuronal commitment, and promotion of glial fates (Wang and Barres 2000; Gaiano and Fishell 2002). Correspondingly, Notch1 is expressed predominantly in proliferating neural progenitor cells in the ventricular zone (VZ) of the embryonic brain (Lindsell *et al.* 1996), and continues to be expressed postnatally in specific regions. However, the activation pattern of Notch1 during neural development for the most part remains unknown, because only very small amounts of N1-ICD are active, and hardly any is detectable in the nucleus *in vivo* (Schroeter *et al.* 1998).

Here, to determine the activation pattern of Notch signaling *in situ*, we performed immunohistochemical analyses of the embryonic and perinatal mouse brain using an antibody specific for the activated form of Notch1, which enhanced the sensitivity of the detection. We found that in the embryonic mouse forebrain, Notch1 was activated in proliferating neural progenitor cells, but not in postmitotic neurons. In the postnatal brain, it was shown that Notch1-activation took place transiently during the astrocytic development.

Materials and methods

Animals and tissue preparation

C57/BL6 mice, used for the preparation of tissue protein extracts and tissue sections, were obtained from Charles River Japan Inc (Kanagawa, Japan). The date of conception was established by the presence of a vaginal plug and recorded as E0.5; the day of birth was designated as postnatal day (P) 0.

cDNA expression constructs

The forms of mouse Notch1 used in this study are summarized in Fig. 1. The expression vector containing mouse full-length Notch1 was kindly provided by Dr J. Nye. N1ΔE was kindly provided by Dr Masato Nakafuku (Yamamoto *et al.* 2001). These cDNAs were subcloned into the pEF-Bos expression vector.

Transfection of cultured cells

The NIH3T3 mouse fibroblast cell line was maintained at 37°C in 5% CO_2. In transient-expression studies, these cells were transfected with cDNAs inserted into pEF-Bos expression vector using the Lipofectamine Plus reagent (Invitrogen, Carlsbad, CA, USA). The cell lines were maintained in Dulbecco's modified Eagle's medium (DMEM) supplemented with 10% fetal calf serum. The cells were incubated for 24 h after the transfection.

γ-Secretase inhibitor treatment

A stock solution of L-685458 (Bachem, King of Prussia, PA, USA) in dimethyl sulfoxide was diluted to 10 μM in phosphate buffered saline (PBS) and injected into embryonic mouse forebrain *exo utero* at E14.5. Control embryos were mock injected with PBS containing the same concentration of DMSO carrier alone. A 2 μL volume of the solution in PBS was injected into the lateral ventricle with a microinjector (Eppendorf, Hamburg, Germany), and 2 days later the embryos were dissected, fixed, and used for immunostaining. The *exo utero* surgery was performed according to the available protocol (Saito and Nakatsuji 2001). In the case of the NIH3T3 cell line, 6 h after transfection the medium was changed to DMEM containing 10 μM L-685458, and the cultured cells were incubated for 16 h before being used for immunostaining. The dose–response analysis was done by immunoblotting.

5-Bromo-2′-deoxyuridine (BrdU) labeling *in vivo*

To label the cells in S-phase, BrdU (Sigma) was injected intraperitoneally into pregnant female at a gestational day from E14.5 [100 μg/g body weight in 200 μL of PBS]. At specific intervals following injection (30 min), embryos were dissected from the uterus and fixed with 4% paraformaldehyde (PFA) in PBS overnight.

Antibodies

Commercially available antibodies: Mouse anti-α-tubulin (Sigma-Aldrich, St. Louis, MO, USA), mouse anti-β-tubulin isotype III (Sigma), mouse anti-glial fibrillary acidic protein (GFAP) (Sigma), goat anti-Notch1 (M-20, Santa Cruz Biotechnology, Inc., Santa Cruz, CA, USA), goat anti-Delta (C-20, Santa Cruz), mouse anti-NeuN (Chemicon, Temecula, CA, USA), rabbit anti-Mash1 (Chemicon), mouse anti-proliferating cell nuclear antigen (PCNA) (Oncogene research product, San Diego, CA, USA), mouse anti-Nestin (Rat401, Developmental Studies Hybridoma Bank; DSHB), rabbit anti-Cleaved-Notch1 (actN1) (Cell Signaling, Beverly, MA, USA), mouse anti-phospho-histone3 (Cell Signaling), mouse anti-Ki67 (Novocastra, Newcastle-upon-Tyne, UK), mouse anti-Mash1 (BD Transduction Laboratories, Los Angeles, CA, USA), mouse anti-glutamine synthetase (GS) (BD Transduction Laboratories), sheep anti-BrdU (Fitzgerald Industries International, Inc., Concord, MA, USA). These antibodies were used according to the manufacturer's protocols. Rabbit anti-Hes1 antibody was provided by Dr T. Sudo (Ito *et al.* 2000), rabbit anti brain lipid binding protein (BLBP) antibody was provided by Dr N. Heintz (Feng and Heintz 1995) and mouse anti-Neurogenin2 was provided by Dr DJ Anderson (Lo *et al.* 2002).

Preparation of cell lysates and immunoblotting

Mouse brain was removed from the skull and dissociated in PBS. An equal volume of 2 × sodium dodecyl sulfate–polyacrylamide gel electrophoresis (SDS–PAGE) sample buffer [100 mM Tris-HCl (pH 6.8, 4% SDS, 20% glycerol, 0.02% bromophenol blue, 12% 2-mercaptoethanol] was added to the lysate and the sample was boiled for 5 min. NIH3T3 cells were collected by centrifugation at 100 × *g* for 5 min. The cell pellets were lysed in 1 × SDS–PAGE sample buffer. Equal loading of the lysate proteins was verified by immunoblotting α-tubulin on a duplicate gel. Tissue and cell lysates were resolved on 7.5% SDS–PAGE gels that were then electroblotted onto Immobilon-P membranes (Millipore, Bedford, MA, USA) with a semi-dry transfer apparatus. The chemiluminescent signals were detected by ECL (Amersham Pharmacia Biotech, Piscataway, NJ, USA) with Kodak X-OMAT film (Kodak, Rochester, NY, USA) according to the manufacturer's instructions.

Immunohistochemistry

We performed immunohistochemical study on tissue sections using three or more independent samples from the mice of different

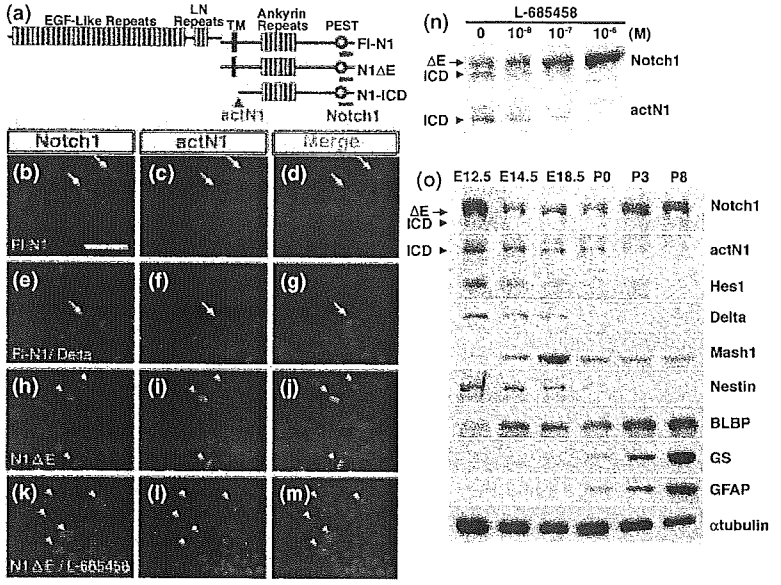

Fig. 1 (a) Schematic representation of the Notch1 protein. cDNAs encoding two forms of Notch1 were assembled: Fl-N1 and N1ΔE. N1-ICD, a form of activated Notch1 processed by S3-site cleavage, is also shown. The respective recognition sites of the anti-Notch1 and actN1 antibodies are also indicated below the schematic drawings. The vertical arrowhead indicates the regions arising from the cleavage. (b–d) NIH3T3 cells that were transfected with Fl-N1 alone showed anti-Notch1-IR (red) in the cell membrane and cytoplasm, but not actN1-IR (green). (e–g) Cells cotransfected with Fl-N1 and Delta showed both Notch1-IR (red) in the cell membrane and cytoplasm, and actN1-IR (green) in the nucleus. (h–j) Cells transfected with N1ΔE, showed strong Notch1 (red) and actN1-IR (green) in the nucleus. (k–m) Cells transfected with N1ΔE and treated with L-685458, a γ-secretase inhibitor, were stained with anti-Notch1-IR (red) but not actN1-IR (green). Nuclei were counterstained with Hoechst (blue). Scale bar: b–m, 50 μm; (n) NIH3T3 cells transfected with N1ΔE were treated with the indicated concentrations of L-685458 for 16 h. Cell lysates were analyzed for N1ΔE (uncleaved) and N1-ICD (cleaved) using the anti-Notch1 and actN1 antibodies. Upper panel, Increasing concentrations of L-685458 led to a build-up of uncleaved Notch1 (120 kDa) by probing the immunoblot with anti-Notch1 antibody. Lower panel, the same fraction was analyzed for the N1-ICD (110 kDa) by sequentially probing the immunoblot with the actN1 antibody. (o) Expression of Notch signaling-related components in the mouse brain. The sizes of N1ΔE (ΔE, arrow) and N1-ICD (ICD, arrowhead) are indicated. α-Tubulin expression was used as a control.

pregnant female. Pups and 8-week-old adult mice were perfused through the left ventricle with 4% PFA in 0.1 M PBS, pH 7.4. Embryos were removed by cesarean section and immediately immersed in the same fixative. Brains were dissected and postfixed overnight at 4°C, cryoprotected in 30% sucrose in PBS overnight at 4°C, then embedded in OCT compound (Tissue Tek; Miles, Elkhart, IN, USA). Cryostat sections (12 μm) were cut and affixed to MAS-coated glass slides (Matsunami Glass, Osaka, Japan). Antigen retrieval was accomplished by autoclave treatment in 0.01 mol/L citrate buffer, pH 6.0, or in Target Retrieval Solution (Dako, Carpinteria, CA, USA), for the anti-Notch1 and Cleaved-Notch1 (actN1) antibodies, at 105°C for 5 min followed by three washes in PBS. The sections were then permeabilized in TBS-T (TBS containing 0.05%Tween20) for 10 min and blocked with 10% normal donkey serum (Chemicon) in PBS for 1 h at room temperature. Subsequently, the sections were incubated overnight at 4°C in a mixture of the primary antibodies described above, in blocking solution. After the sections were washed three times in PBS, they were incubated in a mixture of biotin-conjugated secondary antibodies (Jackson ImmunoResearch, West Grove, PA, USA) for 1 h at room temperature, immersed in 3% H_2O_2 to inactivate endogenous peroxidase at room temperature for 10 min, incubated in the ABC kit mixture (Vector Laboratories, Burlingame, CA, USA), according to the manufacturer's directions, and visualized by the TSA Fluorescein System (PerkinElmer Life sciences, Boston, MA, USA). For double staining, sections were also incubated in a mixture containing the following secondary antibodies for 1 h: Alexa Fluor 488- or 568-conjugated goat anti-mouse, rabbit IgG, or donkey anti-goat IgG (Molecular Probes, Eugene, OR, USA). After being rinsed in PBS, the sections were mounted and examined under a fluorescence microscope (Zeiss Axiophoto) equipped with the appropriate epifluorescence filters. Optical sections were viewed using a scanning-laser confocal imaging system (Zeiss LSM510).

Results

Characterization of Notch1-specific antibodies

To examine the activation patterns of Notch1 *in situ*, we used two commercially available antibodies: anti-Notch1 (M-20) and anti-cleaved Notch1 (actN1). The anti-Notch1 antibody was raised against the C-terminal fragment of the mouse

Notch1 protein, whereas the actN1 antibody recognizes the cleavage site of Notch1, between Gly 1743 and Val 1744, that is generated by presenilin/γ-secretase (see Materials and methods and Fig. 1a). To confirm the specificity of these antibodies, we performed immunocytochemistry and immunoblotting analyses using NIH3T3 cells that were transfected with Notch1 expression vectors.

First, we compared the staining patterns of the actN1 and anti-Notch1 antibodies by immunostaining. NIH3T3 cells were transfected with plasmids encoding full-length mouse Notch1 (Fl-N1) alone or cotransfected with Fl-N1 and Delta (Fig. 1b–g). The anti-Notch1 antibody labeled the cell membrane and cytoplasm of cells that were transfected with Fl-N1 alone but the actN1 antibody did not (Fig. 1b–d), indicating that the Fl-N1 product was not cleaved at the γ-secretase-sensitive site in the absence of an exogenous ligand. However, when NIH3T3 cells were cotransfected with both Fl-N1 and Delta to stimulate Notch signaling in a ligand-dependent manner (Jarriault *et al.* 1998), the major localization sites of Notch1 that were determined by the anti-Notch1 antibody were the cell-membrane and cytoplasm (Fig. 1e), but the cleaved form of Notch1 was detected within the nucleus by the actN1 antibody (Fig. 1f), suggesting that the Fl-N1 product was cleaved in a ligand-dependent manner and then translocated to the nucleus.

To confirm the transactivation of downstream genes by Notch1 in this culture, we introduced a reporter luciferase gene under the control of the *Hes1* promoter (*Hes1*-luc) (Jarriault *et al.* 1995) into NIH3T3 cells by transient transfection. Transactivation of the *Hes1* promoter was observed in cells expressing both Fl-N1 and Delta, but not in cells expressing only Fl-N1 (data not shown). Thus, these results suggest that the expression of both full-length Notch1 and its ligand (Delta) are required for the nuclear localization of activated Notch1 as well as for Hes1-transactivation.

As a positive control, we also analyzed cells transfected with a constitutively active truncated form of Notch1 (N1ΔE) that contained the transmembrane region and the entire ICD. A previous report showed that N1ΔE is a dominant-active form and induces expression of a Notch1 downstream gene (Kopan *et al.* 1996). The N1ΔE products were cleaved by presenilin/γ-secretase in a ligand-independent manner (Fig. 1h-m, described in the next paragraph), producing N1-ICD forms (see Fig. 1a). We also observed the strong transactivation of the *Hes1* promoter in N1ΔE-transfected cells (data not shown). In N1ΔE-transfected cells, Notch1 was clearly detected in the nucleus by both the actN1 (Fig. 1i), and anti-Notch1 (Fig. 1h) antibodies.

To further confirm the specificity of the actN1 antibody for activated Notch1, we investigated the effects of a γ-secretase inhibitor on actN1 immunoreactivity (IR) in NIH3T3 cells transfected with the N1ΔE cDNA. We used a highly specific γ-secretase inhibitor, the L-685458 (Li *et al.* 2000), which blocks Notch endoproteolysis at the γ-secretase-sensitive site. In the presence of this inhibitor, cells transfected with N1ΔE were labeled by the anti-Notch1 antibody but not actN1 antibody (Fig. 1k–m). We also characterized the specificity of the actN1 antibody by immunoblotting. The N1-ICD fragment was readily visible in cells that were not treated with L-685458 by combined immunoblotting with the actN1 and anti-Notch1 antibodies, but the generation of N1-ICD was inhibited by L-685458 treatment (Fig. 1n, upper panel). With increasing concentrations of L-685458, we detected larger amounts of the uncleaved form of Notch1 (120 kDa) with a concomitant decrease in the amount of the cleaved form. Subsequent analysis of the same blot using the actN1 antibody confirmed a dose-dependent reduction in the generation of the cleaved form (110 kDa) by L-685458 treatment (Fig. 1n, lower panel). Collectively, these results show that the actN1 antibody used in the present study can detect the ICD of Notch1 only when it has been cleaved in a γ-secretase-sensitive fashion, but that it does not detect full-length Notch1.

Next, to confirm the specificity of the actN1 antibody for activated Notch1 *in situ*, we investigated the presence of actN1-IR on brain sections obtained at E16.5 from animals that had or had not been injected with γ-secretase inhibitor. In brains injected with PBS alone, nuclear actN1-IR was detected in a subpopulation of the Notch1-IR-positive VZ cells (Fig. 2c,d). The L-685458 treatment did not affect Notch1-IR (Fig. 2e). However, virtually no actN1-IR could be detected in the brain injected with L-685458 (Fig. 2f). These results indicate that the presence of actN1-IR on the brain sections reflects the γ-secretase-dependent activation of Notch1 *in situ*.

Developmental expression of full-length Notch1 and its activated form in the CNS

We, then, examined the activation pattern of Notch1 during mouse brain development by immunoblotting. Uncleaved form of Notch1 (ΔE 120 kDa) was detected from the embryonic stage to the perinatal stage. However, we also detected a strong 110 kDa signal (ICD) in the E12.5 mouse brain using the actN1 antibody, although the activated Notch1 gradually decreased at later stages (Fig. 1o). We also examined the expression of Delta and Hes1 during CNS development. Delta is a Notch ligand and Hes1 is a target of Notch1. They each had almost same expression pattern as activated Notch1 (Fig. 1o). Mash1 is one of the proneural bHLH factors. When cell fate is switched from self-renewal to differentiation, multipotent NSCs generate a transient neuronal precursor cell type, which is defined by the expression of Mash1 (Torii *et al.* 1999). We found that Mash1 showed a complementary expression pattern to activated Notch1 and Hes1, being up-regulated during neurogenesis. Next, we examined the expression patterns of several lineage markers: Nestin, brain lipid binding protein (BLBP), glutamine synthetase (GS), and glial fibrillary acidic

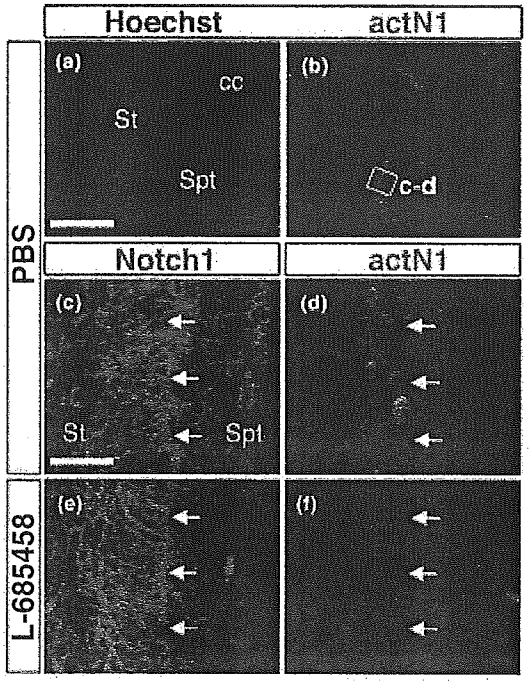

Fig. 2 Characterization of Notch1-specific antibodies by immunohistochemistry. Brain sections at E16.5 were immunostained using anti-Notch1 (red) and actN1 (green) antibodies. (a,b) Activated Notch1 staining (green) was localized to nuclei in the neuroepithelium. This section was counterstained with Hoechst (blue). (c,d) Embryos injected with Mock stained with both anti-Notch1-IR (red) and actN1-IR (green). (e,f) Embryos injected with L-685458 stained with anti-Notch1-IR (red) but not with actN1-IR (green). Arrowheads indicate the ventricle. Striatum (St), septum (Spt) corpus callosum (cc). Scale bars: a,b, 250 μm; c–f, 25 μm.

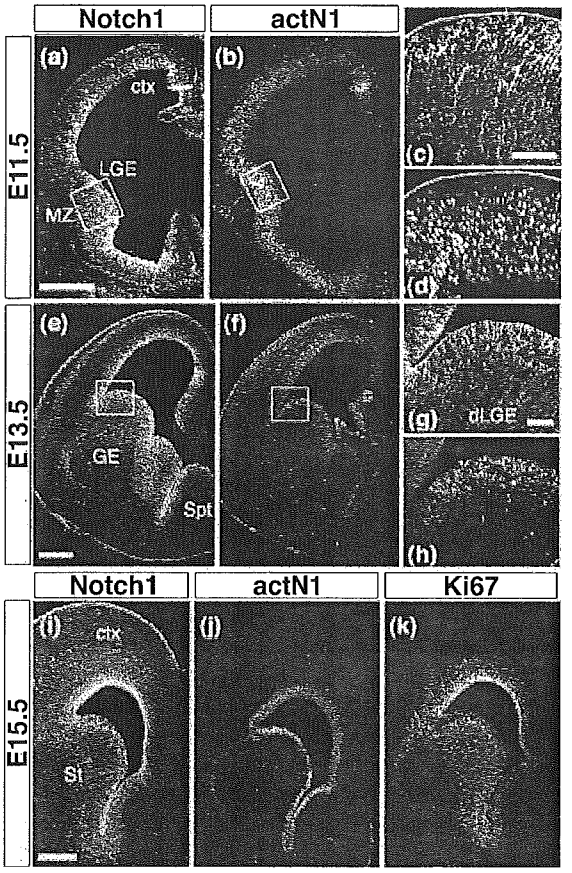

Fig. 3 Immunofluorescence labeling *in situ* throughout the embryonic brain with antibodies against Notch1 (anti-Notch1 and actN1 antibodies). Notch1 was strongly expressed in the neuroepithelium of the basal telencephalic plate, and to a lesser extent in the cortex at E11.5 (a,c) and E13.5 (e,g). Activated Notch1 was localized to the nucleus and strongly expressed in the neuroepithelium of the LGE and septum, but was less strong in the cortex at E11.5 (b,d) and E13.5 (f,h). (i–k) Activated Notch1 was uniformly distributed in anti-Notch1-, anti-Ki67-positive cells in the VZ at E15.5. (c,d) and (g,h) are higher magnification views of the areas boxed in (a,b) and (e,f), respectively. Coronal sections: E11.5 (a–d), E13.5 (e–h), and E15.5 embryos (i–k). Cortex (ctx), lateral ganglionic eminence (LGE), dorsal LGE (dLGE), mantle zone (MZ), striatum (St), septum (Spt). Lateral is to the left, and dorsal is up. Scale bars: a,b, 250 μm; c,d, 50 μm; e,f, 250 μm; g,h, 50 μm; i–k, 250 μm.

protein (GFAP). Nestin is an intermediate filament protein that is expressed in radial glial cells, which have been defined as neural progenitor cells (Hockfield and McKay 1985; Lendahl *et al.* 1990). BLBP is known to be first expressed in radial glial cells, and its expression later becomes restricted to immature astrocytes (Feng *et al.* 1994; Kurtz *et al.* 1994). In the present study, Nestin was expressed during the embryonic stage, but its expression decreased after birth. The expression of BLBP was detected at a later stage than that of Nestin, and BLBP expression gradually increased through the perinatal stage. On the other hand, both astrocyte markers, GS and GFAP, increased with the advancing developmental stage, beginning at around P0 (Fig. 1o).

Next, we used immunohistochemistry to examine the localization of these gene products in the developing brain. Anti-Notch1-IR was found in the VZ of the developing CNS with regional specificity (Fig. 3a,e,i). By E11.5 in the mouse brain, Notch1-IR was strongly detected in the neuroepithelium of the basal telencephalic plate and septum and to a lesser extent in the cortex (Fig. 3a). This is consistent with a previous report of Notch1 expression performed with *in situ* hybridization (Lindsell *et al.* 1996). Moreover, Notch1-IR was localized to the cell membrane (Figs 1b and 3a,c). In contrast, actN1-IR was localized to the nuclei of cells in the VZ at E11.5 (Fig. 3b,d). actN1-IR was strongly detected in the neuroepithelium of the ganglionic eminence (GE) and to a lesser extent in the cortex. Similar to the results for the actN1-immunostaining, a visible difference between the dorsal and ventral telencephalic regions was observed using

anti-Notch1 antibody staining (Fig. 3a,b). However, actN1-IR was not detected at the lumenal surface of the VZ, although the Notch1-IR was strongly detected there (Fig. 3c,d). At E13.5 and E15.5, actN1-positive cells were sparsely distributed among the anti-Notch1-positive cells in the germinal zone of the lateral ganglionic eminence (LGE) and septum (Fig. 3e–j). These results showed that cleavage of Notch1 occurred in a subpopulation of the Notch1-positive proliferating cells in the fetal mouse forebrain. Furthermore, the areas labeled by actN1-IR were part of the Ki67-positive proliferating cells (Fig. 3j,k). At the same stage, actN1-IR was also detected in the midbrain, hindbrain, eye, neural crest, and olfactory epithelium (data not shown).

To examine in more detail the cell types in which Notch1 is activated, we performed double immunohistochemical staining using the actN1 antibody and antibodies against several cell-type-specific markers, followed by comparative confocal microscopic analysis of the cerebral cortex and GE at E11.5 and E14.5. At these stages, Nestin is expressed in the radial glial cells, which are mainly visualized as fibers extending from the ventricular area to the pial surface (Hockfield and McKay 1985; Lendahl *et al.* 1990; Miyata *et al.* 2001; Rakic 2003). Notch1-IR was detected in almost the same area as Nestin (Fig. 4a–c), and the similarity of their localization suggested that the cell membrane was adjacent to the intermediate filaments. Thus, Notch1 is strongly expressed in radial glial cells, In contrast, the actN1-IR-positive cells were a subset of the Nestin- and Notch1-positive cells that lay closer to the ventricular surface (Fig. 4d–g). Nonetheless, the activated Notch1 was not expressed in βIII-tubulin-positive neurons (Fig. 4h). In addition, activated Notch1 labeling was observed in PCNA-positive proliferating cells, within the VZ (Fig. 4i).

It is notable that the actN1-IR was not detected at the lumenal surface of the VZ (Fig. 4j–l), i.e. the site of the mitosis, although the Notch1-IR was present in this area (Fig. 3c,d). Here, we further characterized the Notch1-activation during cell cycle phases. We examined the localization of actNI-IR in the following cell types: (i) the cells labeled by a short (1/2 h) BrdU-pulse that are mostly in S-phase; and (ii) the cells positive for Phospho-histone3 (PH3, a specific marker of mitotic cells), that are in M phase and located at the lumenal surface of the VZ. Interestingly, the actN1-IR correlated with the 1/2 h BrdU-pulse-labeled cells (Fig. 4m), but not with the PH3-positive cells (Fig. 4n) at E14.5. Thus, Notch1 is likely to be activated at least in S phases, but not in M phases. This result indicated that the Notch1-signaling is activated in a cell cycle phase-dependent fashion.

Developmental expression of activated Notch1 and proneural bHLH factors (Mash1 or Neurogenin2) in the early embryonic CNS

Regarding the expression of the two proneuronal bHLH factors in the mouse embryonic forebrain, Mash1 has been shown to be expressed at high levels in ventral neuronal progenitors and at reduced levels in a subset of dorsal neuronal progenitors, contrasting the restricted expression of

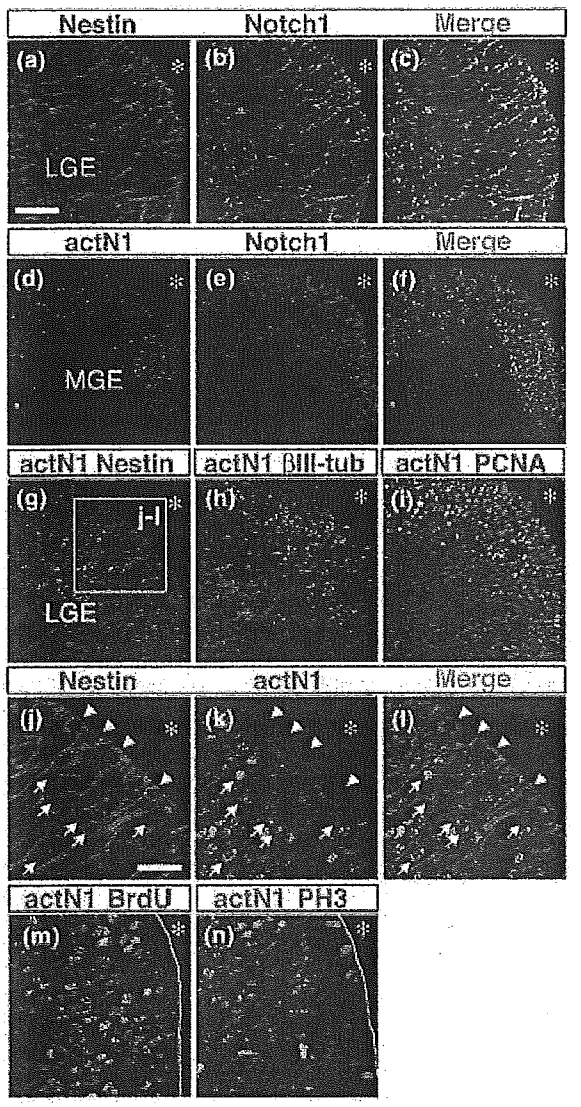

Fig. 4 Expression pattern of activated Notch1 in the developing CNS. (a–c) Brain sections were immunostained using anti-Notch1 (green) and anti-Nestin (red) antibodies. Notch1 was coexpressed with Nestin in the VZ of the basal forebrain. (d–f) Activated Notch1 staining (green) was seen in the Notch1-positive neuroepithelium (red). (g–i), actN1 staining (green) was seen in the Nestin-positive neuroepithelium (g, red). actN1-positive cells were double labeled with PCNA-IR (i, red), but not βIII-tubulin-IR (h, red). (j–l) enlarged image of (g). (m,n) actN1-positive cells were double labeled with BrdU-IR (m, red), but not PH3 (n, red). Arrows depict examples of Nestin- and actN1-double-labeled cells. Arrowheads depict the lumenal surface of the VZ. Coronal sections: E11.5 (a–f), and E14.5 (g–n) embryos. Asterisk: lateral ventricle. Lateral ganglionic eminence (LGE), Medial ganglionic eminence (MGE). Scale bars: a–i, 50 μm; j–n, 25 μm.

Neurogenin2 (Ngn2) in dorsal neuronal progenitors (Fode *et al.* 2000). In addition to responding to the specifications of dorsal-ventral identity, Mash1 and Ngn2 are known to have similar roles in neuronal commitment (Nieto *et al.* 2001). The immunoblot analysis in the present study revealed that the expression profile of Mash1 was complementary to that of activated Notch1 (Fig. 1o). Here, we characterized the relationship between Mash1 or Ngn2-expressing cells and actN1-IR positive cells in greater detail using immunohistochemistry.

First, to examine the features of the Mash1-expressing cells, we performed immunostaining with Mash1 and several lineage markers. In the early embryonic telencephalon at E11.5 and E14.5, Mash1 was expressed in the germinal zone of the GE (Fig. 5a,b). Mash1 expression was colocalized with Nestin (Fig. 5c,d), and there was no overlap with βIII-tubulin (Fig. 5e,f), just as seen with the actN1-IR-positive cells (Fig. 4g,h).

Next, to determine the cell types in which Notch1 is activated in the developing brain, we performed double immunohistochemistry staining using the actN1, Mash1 and Ngn2 antibodies. Mash1 and activated Notch1 were expressed in a complementary fashion at E11.5 and E14.5 in the germinal zone of the GE (Fig. 5g–j). Likewise, Ngn2 and activated Notch1 exhibited complementary expression profiles in the germinal layers of the cortex (Fig. 5k–n). Furthermore, Mash1 or Ngn2 were transiently expressed in Nestin-IR-positive and actN1-IR-negative cells, and the number of cells expressing these bHLH proteins were highest in the VZ throughout neural development (Fig. 5g–n). These results suggest that the Nestin-positive precursor cells in the embryonic forebrain can be classified into two populations that are positive for either activated Notch1 or Mash1/Ngn2, but not both.

Notch1 is activated in the generation of astrocytes in the late embryonic CNS

Notch receptors play crucial roles in many cellular differentiation programs. In addition to the more classical role of Notch in keeping cells in an undifferentiated state (Gaiano *et al.* 2000; Chambers *et al.* 2001; Hitoshi *et al.* 2002), a recent paper has provided *in vitro* and *in vivo* evidences indicating that Notch signaling is a powerful means of directing CNS precursor cells into the glial fate (Gaiano *et al.* 2000; Nye *et al.* 1994; Tanigaki *et al.* 2001).

Therefore, we examined whether Notch1 is activated endogenously in the cells of the astrocytic lineage within the peri-ventricular area at E17.5, P0, and P8, when a high level of gliogenesis occurs (Alvarez-Buylla *et al.* 2001). In recent years, several reports have described the transition from radial glia to astrocytes (Schmechel and Rakic 1979; Voigt

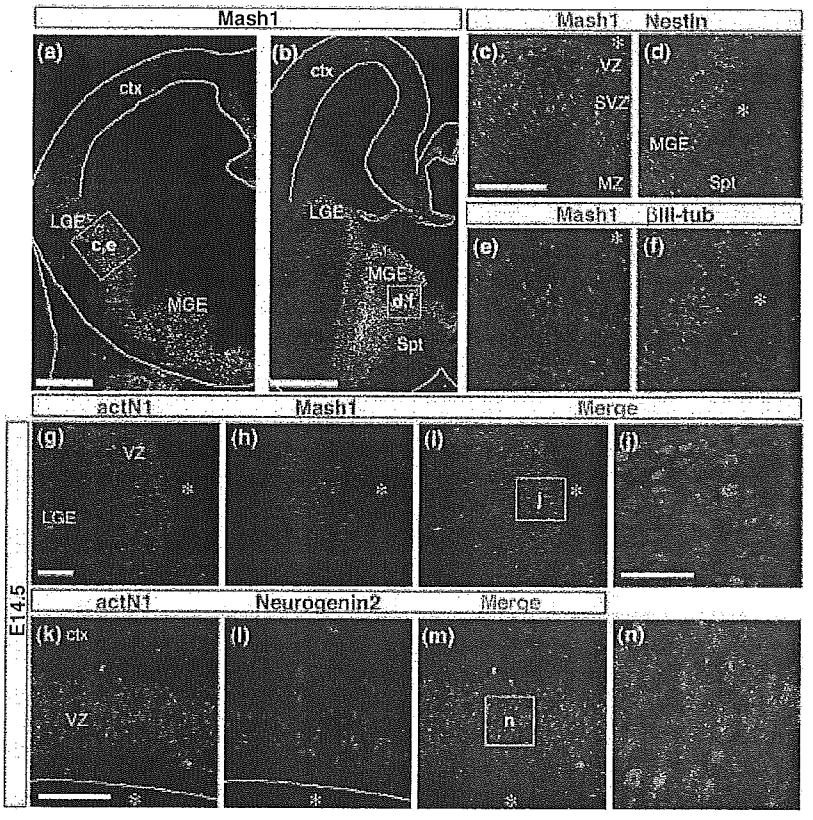

Fig. 5 Activated Notch1 and Mash1 expression patterns show no overlap. Immunostaining images of the anti-Mash1 and Ngn2 antibodies. (a–f) Mash1 was strongly expressed in the neuroepithelium of the basal telencephalic plate. White lines indicate the edge of the tissue at E11.5 (a) and E14.5 (b). Mash1-positive cells (green) were double labeled with Nestin (c, d, red) but not βIII-tubulin (e, f, red) at E11.5 and E14.5. (g–j) Activated Notch1 (green) and Mash1 (red) were expressed at high levels in the neuroepithelium, although the expression patterns were complementary at E14.5. (i) was merged image of (g,h). (j) Higher magnification views of the areas boxed in (i). (k–n) Activated Notch1 (green) and Ngn2 (red) were complementarily expressed in the neuroepithelium of the cortex at E14.5. Coronal sections: E11.5 (a,c,e) and E14.5 (b,d,f,g–n) embryos. Asterisk: lateral ventricle. Cortex (ctx), lateral ganglionic eminence (LGE), medial ganglionic eminence (MGE), septum (Spt), ventricular zone (VZ), subventricular zone (SVZ), mantle zone (MZ). Scale bars: a, 125 μm; b, 250 μm; c–f, 50 μm; g–i,k–m, 50 μm; j,n, 25 μm.

1989). At P0, the majority of cells within the VZ are identified as radial glia. At P8, the proportion of radial glia had decreased while the proportion of immature astrocytes increased. The disappearance of Nestin-positive radial glial cells from the telencephalon correlated with the appearance of GFAP-positive astrocytes (Tramontin *et al.* 2003). Radial glia are thought to give rise to GFAP-positive astrocytes. However, the intermediate cells in this transition (astrocyte precursors) have not been identified in mammalian brains because of the absence of an exclusively specific marker. We immunohistochemically investigated the transition of radial glia to astrocytes using antibodies to several molecules expressed in radial glial and/or astrocytes: BLBP, GS and GFAP. GS is known to be detectable in astrocytes and some radial glial cells (Akimoto *et al.* 1993). The temporal expression profiles of these markers showed some overlap, although the profiles were not identical, during the transition from radial glia to astrocytes. Thus, the putative astrocyte precursors could be estimated using a combination of these markers. In the present observation, we found that BLBP, but not GS, was expressed in radial glia in the VZ at E14.5 (Fig. 6a–c). GS-positive cells appeared in the radial glial cells in the germinal zone of the striatum at E17.5. Interestingly, these GS-positive cells were closely colocalized with BLBP (Fig. 6d–f), but the Mash1 and GS expression patterns did not overlap (Fig. 6g–i). Next, by combining immunostaining for activated Notch1 and astrocytic lineage markers, we found that Notch1-IR stained proliferating progenitor cells in the VZ, which also contained GS-positive cells (Fig. 6j–l). Furthermore, most of the actN1-IR was confined to the VZ in a pattern similar to that seen with GS immunostaining at E17.5 (Fig. 6m–o). At P0, GS-positive cells were found at scattered locations, apparently exhibiting radial migration, and were coexpressed with BLBP in the mantle layer (Fig. 7a–c). The GS-positive cells within the VZ, which were also actN1-IR positive, had small, round cell bodies (Fig. 7d–f); their morphologies were similar to those described previously for glial precursor cells (Levison and Goldman 1993; Levison *et al.* 1993; Zerlin *et al.* 1995). GFAP-positive cells have not yet appeared in the lateral ventricular wall at P0. These cells began to appear at P7, and by P15 GFAP staining is abundant in the lateral ventricular wall (Gates *et al.* 1995; Tramontin *et al.* 2003). In the P8 brain, a subset of putatively migrating glial cells that express GS are sparsely distributed along what are thought to be pathways toward the corpus callosum and cerebral cortex (Tramontin *et al.* 2003). GS-IR was detected in GFAP-positive differentiated astrocytes at P8 (Fig. 7g–i). Thus, GS expression is likely to have occurred in BLBP-positive radial glia and to have remained in GFAP-positive differentiated astrocytes. These results led us to suppose that the GS-positive cells may include astroglial precursor cells. In the P8 brain, a part of actN1-IR was colocalized with GFAP-IR in a region near the VZ (Fig. 7j,k). In addition, actN1-IR almost

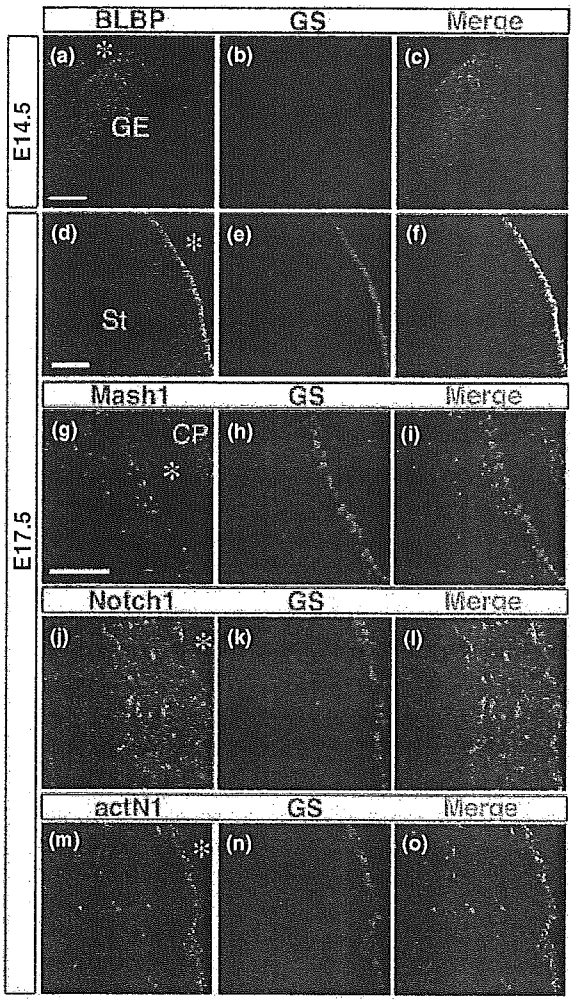

Fig. 6 Activated Notch1 is expressed in GS-positive radial glial cells. (a–c) Brain sections were immunostained with antibodies against BLBP (green) and GS (red). BLBP was expressed in the VZ of the basal forebrain, but GS expression was not observed at E14.5. (d–f) GS (red) was coexpressed with BLBP (green) in the VZ of the striatum at E17.5. (g–i) Dual labeling with Mash1-IR (green) and GS-IR (red) shows no overlapping areas. (j–l) Dual labeling of Notch1 (green) and GS (red) shows overlapping areas. (m–o) Dual labeling of activated Notch1 (green) and GS (red) shows close colocalization. Coronal sections: E14.5 (a–c) and E17.5 (d–o) embryos. Asterisk: lateral ventricle. Ganglionic eminence (GE), striatum (St), choroid plexus (CP). Scale bars: a–c,g–o, 50 μm; d–f, 100 μm.

never labeled dispersed mature fibrous astrocytes expressing GFAP in the white matter (data not shown). These results suggested that Notch1 is strongly activated in the early phase of astroglial differentiation, but is down-regulated during the terminal differentiation of astrocytes.

It should be also interesting to examine the activation profile of Notch1 in the SVZ astrocytes in the adult forebrains (i.e. the adult NSCs) (Doetsch *et al.* 1999). However, we

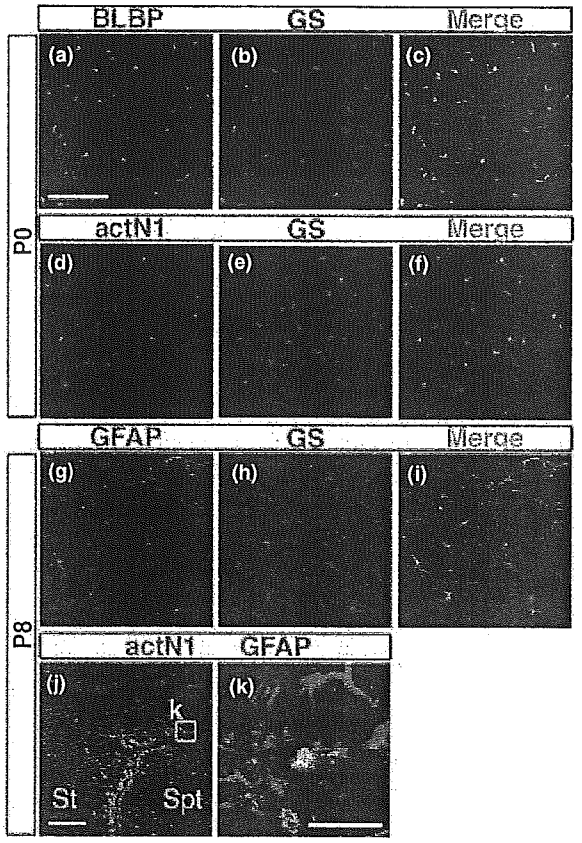

Fig. 7 Notch1 expression is retained in astrocytes. (a–c) The expression pattern of GS (red) was compared with that of BLBP (green) in the P0 forebrain at P0. BLBP and GS double-positive cells were detected in the ventrolateral area of the mantle layer. (d–f) actN1/GS-double-positive astroglial cells were sparsely distributed in the same area shown in (a–c). (g–i) Double immunofluorescence staining at P8 revealed that GS-positive cells also expressed the astrocytic marker GFAP. (j,k) Dual labeling of activated Notch1 (green) and GFAP (red) shows colocalization in the P8 brain. (k) shows higher magnification views of the boxed areas in (j).Coronal sections: P0 (a-f) and P8 (g-k) brains. Asterisk: lateral ventricle. Striatum (St), septum (Spt). Scale bars: a–j, 50 μm; k, 20 μm.

found that the actN1-immunostaing was hardly detectable in the adult forebrain SVZ (data not shown).

Discussion

Visualization of activated Notch1 *in situ*

Although Notch signaling has been reported to play important roles in development, its spatio-temporal activation pattern was unknown during CNS development. Furthermore, the ligand-dependent nuclear translocation of N1-ICD has not been detected immunohistochemically in almost of the organisms examined so far (Fehon *et al.* 1991; Lieber *et al.* 1993; Rebay *et al.* 1993), except for that identified in mouse postmigratory cortical neurons (Sestan *et al.* 1999). However, notably, even in that study, nuclear localization of N1-ICD was not detected in the proliferating precursor cells in the VZ or SVZ of embryonic forebrain (Sestan *et al.* 1999), where Notch1 activation is likely to occur (Gaiano and Fishell 2002). The low level of activated Notch1 in the nucleus is the most likely explanation for why nuclear Notch had not been detected in spite of the functional activation of Notch signaling reported in the above studies (discussed in Schroeter *et al.* 1998; Struhl and Adachi 1998).

To overcome this problem, in the present study we tried to detect endogenous Notch1 expression and its activation pattern immunohistochemically with higher sensitivity. Our present results show that anti-actN1 antibody can specifically detect the activated form of Notch1, and with higher sensitivity than the conventional anti-Notch1 antibody.

Lateral inhibition model of Notch signaling in mammalian CNS

In the present study, to characterize the cell-type specificity of the Notch1-activated cells, we examined various marker molecules expressed in developing CNS. First, we compared the activation pattern of Notch1 with that of Nestin in the embryonic brain. The results showed that at least subsets of Nestin-positive cells with radial glia-like morphology showed nuclear immunoreactivity to actN1 antibody (Fig. 4j–l). Recently, it was shown that radial glia could actually behave as multipotent NSCs that can generate neurons and glia (Kriegstein and Gotz 2003). Consistent with this, previous studies showed that misexpression of the activated form of Notch1 (N1-ICD) in the embryonic mouse brain promotes radial glial identity (Gaiano *et al.* 2000). Thus, activation of endogenous Notch1 signaling may be involved in the acquisition and/or maintenance of radial glial identity.

Next, we characterized the Notch1-activation pattern, especially in its relation to the expression of proneural bHLH gene Mash1 in the germinal zone of the GE. Neuronal precursors in this region express *Mash1,* the murine homolog of the *Drosophila achaete–scute* complex (*AS-C*) (Franco del Amo *et al.* 1993; Guillemot *et al.* 1993). Mash1-positive precursor cells in the GE might correspond mostly to neuronal precursor cells (discussed in Hartfuss *et al.* 2001). Both *Mash1* and *Notch1* mRNA were detected in similar areas during early murine CNS development (Guillemot and Joyner 1993). Interestingly, however, the Mash1-positive cell populations did not overlap with the activated Notch1-positive cells, as shown in Fig. 5. These results suggest that the activation of Notch1 normally inhibits the expression of Mash1, just as it inhibits the expression of *AS-C* in *Drosophila.* In *Drosophila,* proteins encoded by the *AS-C* genes up-regulate Delta expression in neuronal precursors (i.e. neuroblasts) (Kunisch *et al.* 1994). In addition, Notch activation during lateral inhibition results in the down-regulation of both *AS-C* and Delta expression (Lewis 1996).

In mammalian CNS, newly generated neurons up-regulate the expression of Delta as they differentiate (Casarosa *et al.* 1999). Taken together, these observations suggest that *AS-C* homologs, such as Mash1, may regulate the murine DSL genes (Ma *et al.* 1997). Given that Mash1 is required for neurogenesis in the developing mouse brain, the overlapping expression of Notch1, Delta1, and Mash1 in this region strengthens the idea that these genes participate in a common pathway (Lindsell *et al.* 1996). Thus, tracking the expression of Mash1 may also be a way to monitor the expression of Notch ligands. Mash1-positive cells, which probably express higher amount of Notch ligands, and actN1-positive cells, in which the Notch signaling is activated, were close neighbors, although there was never any overlap in the immunostaining for these molecules (Fig. 5). This result indicates that lateral inhibition might function in these cells.

The Mash1-positive cells in the embryonic GE are known to be precursors for GABAnergic neurons (Kriegstein and Gotz 2003; Malatesta *et al.* 2003; Ross *et al.* 2003). Thus, an attractive model would be that the differential activation of Notch1 in the GE, possibly through lateral inhibition, results in the divergence of two different precursors: precursors for GABAergic neurons (Mash1-positive and actN1-negative) and radial glia committed to an astroglial fate (Mash1-negative and actN1-positive). In addition, Ngn2 is predicted to have the same function as Mash1 in the embryonic cortex, based on the complementary expression of Ngn2 and actN1.

Notch1 activation in glial lineage cells during perinatal CNS development

Recently, it is suggested that Notch1 signaling is Involved in the maintenance of progenitor cells (Artavanis-Tsakonas *et al.* 1999), including progenitors destined to a neuronal fate (Nakamura *et al.* 2000), in an undifferentiated state as well as the promotion of glial fates in mammalian CNS development (Tanigaki *et al.* 2001). The temporal pattern of Notch1 expression differed between neuronal and glial cells; the neuronal expression of Notch1 diminished after the progenitor cells differentiated into neurons (Fig. 4h). Although there has been some debate (Wang and Barres 2000; Gaiano and Fishell 2002; Sun *et al.* 2003), the role of Notch signaling is not completely understood in glial development.

A previous study, in which the activated form of Notch1 was overexpressed in rat adult hippocampus-derived multipotent progenitors, suggests an instructive role for Notch signaling to promote astrocytic fate (Tanigaki *et al.* 2001). In this gain-of-function study *in vitro*, they showed that transient activation of Notch1 (4-hydroxytamoxifen-induced nuclear transport of N1-ICD that had been fused to the estrogen receptor) is sufficient to promote astrocytic fate. To clarify the *in vivo* significance of this finding, it was important to characterize the temporal activation of Notch1 signaling during glial development *in vivo*.

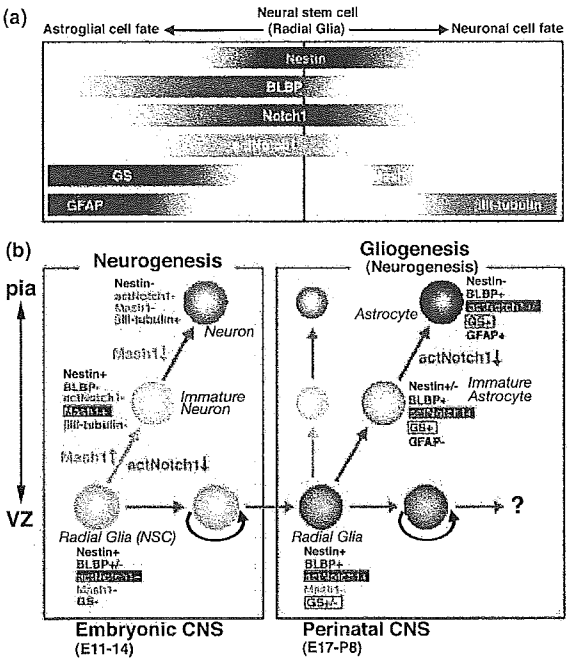

Fig. 8 Model for the expression and function of Notch1 signaling during CNS development. (a) Sequential expression patterns of activated Notch1, Mash1, and several lineage markers during the histogenesis of the CNS. The expressions of activated Notch1, Notch1, Mash1, Nestin, BLBP, GS, GFAP, and βIII-tubulin are initiated in the order given, as development proceeds from neurogenesis to gliogenesis and to neural cell maturation. This scheme includes the results shown in the Table, where mutually overlapping and/or exclusive expression patterns among these antigens are described. (b) Schematic representation of the activation of Notch signaling during embryonic and perinatal CNS development.

In the present study, the glial expression of Notch1 continued even after glial cells became positive for GFAP (Fig. 7k). However, we found that activation of Notch1 was not continuous (data not shown). At least two stages can be distinguished in glial differentiation, as described here (Fig. 8b, right). In the first stage, immature glia express little or none of the glial marker GFAP, but they express significant levels of GS. The immature glia also express activated Notch1 at a high level. In the second stage of glial differentiation, the maturing glia expressed GFAP and was shown little or no Notch1 activation (Figs 7 and 8b). The molecular mechanism responsible for the transient activation of Notch1, resulting in the astrocytic differentiation of neural stem/progenitor cells, remains to be elucidated. However, a recent study has indicated that the corepressor NcoR inhibits the astrocytic differentiation of neural stem/progenitor cells and represses the transcription of the *GFAP* gene by physically interacting with a DNA-binding protein, CSL, that binds directly to the repressor region of the *GFAP* promoter (Hermanson *et al.* 2002; Ge *et al.* 2002). On the

other hand, upon Notch1 activation, N1-ICD translocates into the nucleus to form a complex with CSL (Kato *et al.* 1997), thereby changing CSL from a transcriptional repressor into an activator and stimulating the transcription of its target genes (Beatus *et al.* 2001). Thus, an attractive model would be that the transient activation of Notch1 might de-repress *GFAP* transcription by recruiting N1-ICD into the CSL complex through the exclusion of NcoR from the CSL complex bound to the *GFAP* promoter. Consistent with this theory, the removal of NCoR is indeed sufficient to induce *GFAP* expression *in vivo* and *in vitro* (Hermanson *et al.* 2002). However, whether the transcriptional activator complex, including N1-ICD and CSL, is maintained on the *GFAP* promoter during the maturation of astrocytes must be determined by detailed molecular studies. Future studies concomitantly characterizing the functions of the above-mentioned transcriptional regulators and *in situ* detection of the activated form of Notch1 described in the present study would reveal the significance of the context-dependent actions of Notch signaling.

Acknowledgements

We thank Tetsuo Sudo for rabbit anti-Hes1 antibody, Nathaniel Heintz for rabbit anti-BLBP antibody and David J. Anderson for mouse anti-Neurogenin2. We are grateful to Drs Yukiko Gotoh, Ola Hermanson, Takuya Shimazaki and Shin-ichi Sakakibara for critical comments to this manuscript. This work was supported by grants to HO from the Japanese Ministry of Education, Culture, Sports, Science and Technology, from Japan Science and Technology Agency (CREST), and by a grant-in-aid from the 21th century COE program of the Ministry of Education, Science and Culture to Keio University.

References

Akimoto J., Itoh H., Miwa T. and Ikeda K. (1993) Immunohistochemical study of glutamine synthetase expression in early glial development. *Brain Res. Dev. Brain Res.* **72**, 9–14.

Alvarez-Buylla A., Garcia-Verdugo J. M. and Tramontin A. D. (2001) A unified hypothesis on the lineage of neural stem cells. *Nat. Rev. Neurosci.* **2**, 287–293.

Anderson D. J. (2001) Stem cells and pattern formation in the nervous system: the possible versus the actual. *Neuron* **30**, 19–35.

Artavanis-Tsakonas S., Rand M. D. and Lake R. J. (1999) Notch signaling: cell fate control and signal integration in development. *Science* **284**, 770–776.

Beatus P. and Lendahl U. (1998) Notch and neurogenesis. *J. Neurosci. Res.* **54**, 125–136.

Beatus P., Lundkvist J., Oberg C., Pedersen K. and Lendahl U. (2001) The origin of the ankyrin repeat region in Notch intracellular domains is critical for regulation of HES promoter activity. *Mech. Dev.* **104**, 3–20.

Casarosa S., Fode C. and Guillemot F. (1999) Mash1 regulates neurogenesis in the ventral telencephalon. *Development* **126**, 525–534.

Chambers C. B., Peng Y., Nguyen H., Gaiano N., Fishell G. and Nye J. S. (2001) Spatiotemporal selectivity of response to Notch1 signals in mammalian forebrain precursors. *Development* **128**, 689–702.

Doetsch F., Caille I., Lim D. A., Garcia-Verdugo J. M. and Alvarez-Buylla A. (1999) Subventricular zone astrocytes are neural stem cells in the adult mammalian brain. *Cell* **97**, 703–716.

Fehon R. G., Johansen K., Rebay I. and Artavanis-Tsakonas S. (1991) Complex cellular and subcellular regulation of notch expression during embryonic and imaginal development of Drosophila: implications for notch function. *J. Cell Biol.* **113**, 657–669.

Feng L. and Heintz N. (1995) Differentiating neurons activate transcription of the brain lipid-binding protein gene in radial glia through a novel regulatory element. *Development* **121**, 1719–1730.

Feng L., Hatten M. E. and Heintz N. (1994) Brain lipid-binding protein (BLBP): a novel signaling system in the developing mammalian CNS. *Neuron* **12**, 895–908.

Fode C., Ma Q., Casarosa S., Ang S. L., Anderson D. J. and Guillemot F. (2000) A role for neural determination genes in specifying the dorsoventral identity of telencephalic neurons. *Genes Dev.* **14**: 67–80.

Franco del Amo F., Gendron-Maguire M., Swiatek P. J. and Gridley T. (1993) Cloning, sequencing and expression of the mouse mammalian achaete-scute homolog 1 (MASH1). *Biochim. Biophys. Acta* **1171**, 323–327.

Gaiano N. and Fishell G. (2000) Notch1 signaling promotes the formation of bFGF–responsive neurospheres derived from embryonic mouse telencephalon. *Society of Neuroscience 31st Annual Meeting (Abstract)* **26**, 1347.

Gaiano N. and Fishell G. (2002) The role of notch in promoting glial and neural stem cell fates. *Annu. Rev. Neurosci.* **25**, 471–490.

Gaiano N., Nye J. S. and Fishell G. (2000) Radial glial identity is promoted by Notch1 signaling in the murine forebrain. *Neuron* **26**, 395–404.

Gates M. A., Thomas L. B., Howard E. M., Laywell E. D., Sajin B., Faissner A., Gotz B., Silver J. and Steindler D. A. (1995) Cell and molecular analysis of the developing and adult mouse subventricular zone of the cerebral hemispheres. *J. Comp. Neurol.* **361**, 249–266.

Ge W., Martinowich K., Wu X., He F., Miyamoto A., Fan G., Weinmaster G. and Sun Y. E. (2002) Notch signaling promotes astrogliogenesis via direct CSL-mediated glial gene activation. *J. Neurosci. Res.* **69**, 848–860.

Guillemot F. and Joyner A. L. (1993) Dynamic expression of the murine Achaete-Scute homologue Mash-1 in the developing nervous system. *Mech. Dev.* **42**, 171–185.

Guillemot F., Lo L. C., Johnson J. E., Auerbach A., Anderson D. J. and Joyner A. L. (1993) Mammalian achaete-scute homolog 1 is required for the early development of olfactory and autonomic neurons. *Cell* **75**, 463–476.

Hartfuss E., Galli R., Heins N. and Gotz M. (2001) Characterization of CNS precursor subtypes and radial glia. *Dev. Biol.* **229**, 15–30.

Hermanson O., Jepsen K. and Rosenfeld M. G. (2002) N-CoR controls differentiation of neural stem cells into astrocytes. *Nature* **419**, 934–939.

Hitoshi S., Alexson T., Tropepe V., Donoviel D., Elia A. J., Nye J. S., Conlon R. A., Mak T. W., Bernstein A. and van der Kooy D. (2002) Notch pathway molecules are essential for the maintenance, but not the generation, of mammalian neural stem cells. *Genes Dev.* **16**, 846–858.

Hockfield S. and McKay R. D. (1985) Identification of major cell classes in the developing mammalian nervous system. *J. Neurosci.* **5**, 3310–3328.

Ishibashi M., Ang S. L., Shiota K., Nakanishi S., Kageyama R. and Guillemot F. (1995) Targeted disruption of mammalian hairy and Enhancer of split homolog-1 (HES-1) leads to up-regulation of neural helix-loop-helix factors, premature neurogenesis, and severe neural tube defects. *Genes Dev.* **9**, 3136–3148.

Ito T, Udaka N, Yazawa T, Okudela K, Hayashi H, Sudo T, Guillemot F, Kageyama R. and Kitamura H (2000) Basic helix-loop-helix transcription factors regulate the neuroendocrine differentiation of fetal mouse pulmonary epithelium. *Development* **127**, 3913–3921.

Jarriault S., Brou C., Logeat F., Schroeter E. H., Kopan R. and Israel A. (1995) Signalling downstream of activated mammalian Notch. *Nature* **377**, 355–358.

Jarriault S., Le Bail O., Hirsinger E., Pourquie O., Logeat F., Strong C. F., Brou C., Seidah N. G. and Isra 1 A. (1998) Delta-1 activation of notch-1 signaling results in HES-1 transactivation. *Mol. Cell Biol.* **18**, 7423–7431.

Kageyama R. and Nakanishi S. (1997) Helix-loop-helix factors in growth and differentiation of the vertebrate nervous system. *Curr. Opin. Genet. Dev.* **7**, 659–665.

Kato H., Taniguchi Y., Kurooka H., Minoguchi S., Sakai T., Nomura-Okazaki S., Tamura K. and Honjo T. (1997) Involvement of RBP-J in biological functions of mouse Notch1 and its derivatives. *Development* **124**, 4133–4141.

Kopan R., Schroeter E. H., Weintraub H. and Nye J. S. (1996) Signal transduction by activated mNotch: importance of proteolytic processing and its regulation by the extracellular domain. *Proc. Natl Acad. Sci. USA* **93**, 1683–1688.

Kriegstein A. R. and Gotz M. (2003) Radial glia diversity: a matter of cell fate. *Glia* **43**, 37–43.

Kunisch M., Haenlin M. and Campos-Ortega J. A. (1994) Lateral inhibition mediated by the Drosophila neurogenic gene delta is enhanced by proneural proteins. *Proc. Natl Acad. Sci. USA* **91**, 10139–10143.

Kurtz A., Zimmer A., Schnutgen F., Bruning G., Spener F. and Muller T. (1994) The expression pattern of a novel gene encoding brain-fatty acid binding protein correlates with neuronal and glial cell development. *Development* **120**, 2637–2649.

Lendahl U., Zimmerman L. B. and McKay R. D. (1990) CNS stem cells express a new class of intermediate filament protein. *Cell* **60**, 585–595.

Levison S. W., Chuang C., Abramson B. J. and Goldman J. E. (1993) The migrational patterns and developmental fates of glial precursors in the rat subventricular zone are temporally regulated. *Development* **119**, 611–622.

Levison S. W. and Goldman J. E. (1993) Both oligodendrocytes and astrocytes develop from progenitors in the subventricular zone of postnatal rat forebrain. *Neuron* **10**, 201–212.

Lewis J. (1996) Neurogenic genes and vertebrate neurogenesis. *Curr. Opin. Neurobiol.* **6**, 3–10.

Li Y. M., Xu M., Lai M. T., Huang Q. *et al.* (2000) Photoactivated gamma-secretase inhibitors directed to the active site covalently label presenilin 1. *Nature* **405**, 689–694.

Lieber T., Kidd S., Alcamo E., Corbin V. and Young M. W. (1993) Antineurogenic phenotypes induced by truncated Notch proteins indicate a role in signal transduction and may point to a novel function for Notch in nuclei. *Genes Dev.* **7**, 1949–1965.

Lindsell C. E., Boulter J., diSibio G., Gossler A. and Weinmaster G. (1996) Expression patterns of Jagged, Delta1, Notch1, Notch2, and Notch3 genes identify ligand-receptor pairs that may function in neural development. *Mol. Cell. Neurosci.* **8**, 14–27.

Lo L., Dormand E., Greenwood A. and Anderson D. J. (2002) Comparison of the generic neuronal differentiation and neuron subtype specification functions of mammalian achaete-scute and atonal homologs in cultured neural progenitor cells. *Development* **129**, 1553–1567.

Ma Q., Sommer L., Cserjesi P. and Anderson D. J. (1997) Mash1 and neurogenin1 expression patterns define complementary domains of neuroepithelium in the developing CNS and are correlated with regions expressing notch ligands. *J. Neurosci.* **17**, 3644–3652.

Malatesta P., Hack M. A., Hartfuss E., Kettenmann H., Klinkert W., Kirchhoff F. and Gotz M. (2003) Neuronal or glial progeny: regional differences in radial glia fate. *Neuron* **37**, 751–764.

Miyata T., Kawaguchi A., Okano H. and Ogawa M. (2001) Asymmetric inheritance of radial glial fibers by cortical neurons. *Neuron* **31**, 727–741.

Nakamura Y., Sakakibara S., Miyata T., Ogawa M., Shimazaki T., Weiss S., Kageyama R. and Okano H. (2000) The bHLH gene hes1 as a repressor of the neuronal commitment of CNS stem cells. *J. Neurosci.* **20**, 283–293.

Nieto M., Schuurmans C., Britz O. and Guillemot F. (2001) Neural bHLH genes control the neuronal versus glial fate decision in cortical progenitors. *Neuron* **29**, 401–413.

Nye J. S., Kopan R. and Axel R. (1994) An activated Notch suppresses neurogenesis and myogenesis but not gliogenesis in mammalian cells. *Development* **120**, 2421–2430.

Okano H. (2002) Stem cell biology of the central nervous system. *J. Neurosci. Res.* **69**, 698–707.

de la Pompa J. L., Wakeham A., Correia K. M. *et al.* (1997) Conservation of the Notch signalling pathway in mammalian neurogenesis. *Development* **124**, 1139–1148.

Qian X., Shen Q., Goderie S. K., He W., Capela A., Davis A. A. and Temple S. (2000) Timing of CNS cell generation: a programmed sequence of neuron and glial cell production from isolated murine cortical stem cells. *Neuron* **28**, 69–80.

Rakic P. (2003) Elusive radial glial cells: historical and evolutionary perspective. *Glia* **43**, 19–32.

Rebay I., Fehon R. G. and Artavanis-Tsakonas S. (1993) Specific truncations of *Drosophila* Notch define dominant activated and dominant negative forms of the receptor. *Cell* **74**, 319–329.

Ross S. E., Greenberg M. E. and Stiles C. D. (2003) Basic helix-loop-helix factors in cortical development. *Neuron* **39**, 13–25.

Saito T. and Nakatsuji N. (2001) Efficient gene transfer into the embryonic mouse brain using *in vivo* electroporation. *Dev. Biol.* **240**, 237–246.

Schmechel D. E. and Rakic P. (1979) Arrested proliferation of radial glial cells during midgestation in rhesus monkey. *Nature* **277**, 303–305.

Schroeter E. H., Kisslinger J. A. and Kopan R. (1998) Notch-1 signalling requires ligand-induced proteolytic release of intracellular domain. *Nature* **393**, 382–386.

Selkoe D. and Kopan R. (2003) Notch and presenilin: regulated intramembrane proteolysis links development and degeneration. *Annu. Rev. Neurosci.* **26**, 565–597.

Sestan N., Artavanis-Tsakonas S. and Rakic P. (1999) Contact-dependent inhibition of cortical neurite growth mediated by notch signaling. *Science* **286**, 741–746.

Struhl G. and Adachi A. (1998) Nuclear access and action of notch *in vivo*. *Cell* **93**, 649–660.

Sun Y., Nadal-Vicens M., Misono S., Lin M. Z., Zubiaga A., Hua X., Fan G. and Greenberg M. E. (2001) Neurogenin promotes neurogenesis and inhibits glial differentiation by independent mechanisms. *Cell* **104**, 365–376.

Sun Y. E., Martinowich K. and Ge W. (2003) Making and repairing the mammalian brain – signaling toward neurogenesis and gliogenesis. *Semin. Cell Dev. Biol.* **14**, 161–168.

Tanigaki K., Nogaki F., Takahashi J., Tashiro K., Kurooka H. and Honjo T. (2001) Notch1 and Notch3 instructively restrict bFGF-responsive multipotent neural progenitor cells to an astroglial fate. *Neuron* **29**, 45–55.

Torii M., Matsuzaki F., Osumi N., Kaibuchi K., Nakamura S., Casarosa S., Guillemot F. and Nakafuku M. (1999) Transcription factors Mash-1 and Prox-1 delineate early steps in differentiation of neural stem cells